Cohesive crack with rate-dependent opening and viscoelasticity: I. mathematical model and scaling

ZDENĚK P. BAŽANT[*] and YUAN-NENG LI[**]
Department of Civil Engineering, Northwestern University, Evanston, Illinois 60208, USA

Abstract. The time dependence of fracture has two sources: (1) the viscoelasticity of material behavior in the bulk of the structure, and (2) the rate process of the breakage of bonds in the fracture process zone which causes the softening law for the crack opening to be rate-dependent. The objective of this study is to clarify the differences between these two influences and their role in the size effect on the nominal strength of stucture. Previously developed theories of time-dependent cohesive crack growth in a viscoelastic material with or without aging are extended to a general compliance formulation of the cohesive crack model applicable to structures such as concrete structures, in which the fracture process zone (cohesive zone) is *large*, i.e., cannot be neglected in comparison to the structure dimensions. To deal with a large process zone interacting with the structure boundaries, a boundary integral formulation of the cohesive crack model in terms of the compliance functions for loads applied anywhere on the crack surfaces is introduced. Since an unopened cohesive crack (crack of zero width) transmits stresses and is equivalent to no crack at all, it is assumed that at the outset there exists such a crack, extending along the entire future crack path (which must be known). Thus it is unnecessary to deal mathematically with a moving crack tip, which keeps the formulation simple because the compliance functions for the surface points of such an imagined preexisting unopened crack do not change as the actual front of the opened part of the cohesive crack advances. First the compliance formulation of the cohesive crack model is generalized for aging viscoelastic material behavior, using the elastic-viscoelastic analogy (correspondence principle). The formulation is then enriched by a rate-dependent softening law based on the activation energy theory for the rate process of bond ruptures on the atomic level, which was recently proposed and validated for concrete but is also applicable to polymers, rocks and ceramics, and can be applied to ice if the nonlinear creep of ice is approximated by linear viscoelasticity. Some implications for the characteristic length, scaling and size effect are also discussed. The problems of numerical algorithm, size effect, roles of the different sources of time dependence and rate effect, and experimental verification are left for a subsequent companion paper.

Key words: Fracture mechanics, nonlinear fracture, quasibrittle fracture, cohesive crack, crack bridging, rate effect, time effect, creep, viscoelasticity, characteristic length, scaling, concrete.

1. Introduction

Although the classical fracture mechanics treats fracture as time independent, the process of bond breakages at the fracture front is rate dependent. This needs to be taken into account not only for dynamic fracture, which has been intensely studied for a long time (Freund, 1990), but also for static fracture when very different loading rates and durations are compared. For instance, the time dependence of fracture is important for earthquake analysis of a concrete dam in which cracks have grown slowly for many years due to volume changes and foundation settlements. The dynamic fracture is complicated by the fact that, aside from the rate dependence of the bond breakages at the fracture front, the inertia effects in the vicinity of fracture front and wave propagation play an important role. This study will deal exclusively with static fracture, for which this complication is removed.

---

[*] Walter P. Murphy Professor of Civil Engineering and Materials Science
[**] Research Scientist in the Rank of Assistant Professor

For materials such as concrete, ice or polymers, however, another complication is brought about by need to take into account the creep or viscoelasticity of the material. For polymers, except glassy polymers, the creep appears to be a more important source of time-dependence than the rate dependence of bond breakages at the fracture front, and for elastomers a case can be made that the rate dependence of bond breakage can be altogether neglected in comparison to creep (Knauss, 1989). For rocks and ceramics at room temperature, the creep can be neglected but the rate dependence of bond breakages cannot. For concrete as well as ice, these two distinct physical sources of time dependence are both important.

The time dependence of fracture has in the past been studied chiefly for the materials in which the fracture process zone size is negligible relative to the structure size. This cannot be assumed for quasibrittle materials with coarse heterogeneous microstructure, for example concrete and many rocks. In these materials, the time-dependent generalization must be based on models that take the existence of a long fracture process zone into account.

In the simplest way, this can be done by the so-called R-curve model in which the fracture energy (or fracture toughness) is assumed to be a certain function of the crack length, depending also on specimen geometry. On the basis of the elastic-viscoelastic analogy, the R-curve model has recently been generalized to time-dependent fracture behavior coupled with the effect of linear aging creep in the bulk of the specimen (Bažant and Jirásek, 1993). As has been shown, this model can simulate the effect of loading rate on the load-displacement curves, and particularly on the maximum load. It can also describe the effect of loading rate on the size effect in fracture, especially on the plots of nominal structure strength versus structure size when geometrically similar structures are considered.

The R-curve model, which is essentially an equivalent linear elastic fracture model, is however insufficient for situations where the fracture process zone is so large that it interacts with the specimen boundaries. A fracture model that can handle such situations is the cohesive (or fictitious) crack model, which was initially proposed by Barenblatt (1959; 1962; 1970) and Dugdale (1960), pioneered for concrete by Hillerborg et al. (1976), and investigated in detail by Petersson (1981). Recently, Kanstad (1990) and Zhou (1992) proposed to generalize this model to time-dependent behavior of concrete by modifying the stress-displacement relation for a cohesive crack in a manner analogous to linear viscoelasticity, as modeled by springs and dashpots. Simulations of test results for concrete, however, reveal that a linear approximation to the time-dependence of the stress-displacement relation is insufficient to describe the real behavior of concrete over a broad range of crack opening rates. The crack bridging stress is a highly nonlinear function of the crack opening rate and the crack opening (1993).

The time-dependence of fracture has first been studied for viscoelastic polymers, particularly the filled elastomers (solid rocket propellants), and important results have been obtained. Many studies were based on the assumption that the process zone is infinitesimal compared to the characterisitic dimension of the specimen. Based on the elastic-viscoelastic analogy (or the correspondence principle), Williams (1963) described the viscoelastic effect on the crack propagation considering a viscoelastic model for the material in front of the crack tip. Later, Williams (1963; 1964; 1965) developed a theory for predicting the fracture initiation time and the mode I crack growth in linear viscoelastic media, and established the essential dependence of fracture initiation time and initial crack velocity on the applied loading history. Nuismer (1974) presented an interesting discussion of the power balance equations used in linear viscoelastic fracture mechanics. Willis (1967) analyzed the constant velocity growth of an infinitely long crack in an infinite body made of standard viscoelastic material.

Knauss (1970; 1989; 1993) considered the crack opening displacement to be determined by the (nonaging) viscoelastic properties of the bulk material, and the crack resistance to be represented by the normal traction (cohesive stress). Aside from the simpler case when the distribution of the cohesive stresses over a small fracture process zone can be fixed advance, Knauss (1989; 1993) also treated the general case of a small fracture process zone (or a finite process zone in an infinite solid) in which the cohesive stress distribution is unknown, and analyzed also the energy absorption. Knauss' approach extended to viscoelastic materials the cohesive crack model in the sense of Barenblatt (1962), originally proposed for time-independent fracture behavior. Knauss and Losi (1993) formulated the cohesive crack model with a small fracture process zone for a certain type of nonlinearly viscoelastic material and presented an iterative numerical solution. Schapery (1984) (see also Schapery (1975, 1978, 1980, 1982, 1989)) presented solutions using a general cohesive crack model with variable cohesive stress not restricted to a small fracture process zone, and including viscoelasticity and aging in the surrounding material. Assuming the cohesive stress to be a function of crack opening displacement, McCartney (1988) formulated a nonlinear fracture model for viscoelastic material and demonstrated that the process zone length as well as the distribution of the cohesive stress can vary significantly with the crack speed. Further valuable contributions on time-dependent fracture of solid rocket propellants have been made by Hufferd (1975) and Laheru (1980). Excellent reviews of further literature can be found in Hufferd (1975), Knauss (1993), Schapery (1982, 1984), Lahern (1980), and Petersson (1981).

The present study assumes the material to exhibit viscoelasticity with aging and is based on a nonlinear version of the cohesive crack model, in which the cohesive stress is related to crack opening displacement by a unique softening law and the condition of zero stress intensity factor at the tip of the cohesive zone is enforced. The process zone is considered to be finite, interacting with the structure boundaries, which is handled by introducing the compliance functions of the structure for loads applied on the crack surfaces. Both the initial process zone growth and steady-state crack propagation can be simulated. The basic objective of this and the subsequent companion paper is to study and clarify the different roles of the rate dependence of crack opening and the viscoelasticity of the material, especially their roles in the size effect.

The crack band theory developed by Bažant and Oh (1983) (see also Bažant and Cedolin (1991)) is analogous and essentially equivalent to Hillerborg's cohesive crack model for concrete, and it gives practically the same results. The main difference lies in the modeling of the process zone, which is assumed to have a given finite width h. The cracking strain $\varepsilon_{\mathrm{cr}}$ in the band is equivalent to the opening w of the cohesive crack if one sets $\varepsilon_{\mathrm{cr}} = w/h$. Different (but not too large) values of h can be chosen if the softening stress-displacement curve is scaled according to h so as to make the area under this curve equal to the fracture energy G_f.

The crack band approach is advantageous for numerical implementations (de Borst, 1987), because it allows a crack to be treated the same way as other nonlinear stress-strain relations, such as those for plasticity and creep. Based on this idea, Bažant and Chern (1985) formulated the crack band model with both linear aging creep and rate-dependent softening, although the law they used for the latter was not adequate for a broad range of crack opening rates. A realistic rate-dependent softening law based on the activation energy of the rate-process of bond rupture on the atomic scale was developed by Bažant (1993) and Wu and Bažant (1993). The same model is adopted and refined in this paper.

The crack band model has also been generalized for the rate effect on crack opening in concrete by Kanstad (1990), and in a nonlocal form by Bažant and Ožbolt (1990), but these

generalizations, too, were of limited validity because they used rate-dependent constitutive relations which applied to only a limited retardation spectrum and worked only for one order of magnitude of the crack opening rate or loading rate. It is in fact characteristic of materials such as concrete that the loading rate effect is observed to be significant over many orders of magnitude of the loading rate.

Another advantage of crack band model is that the condition of zero stress intensity factor is absent, but the penalty is that a line crack cannot be simulated exactly. The same is true of the version of cohesive crack model recently introduced by Tvergaard and Hutchinson (1992; 1994), in which a line of continuously distributed springs is assumed to exist ahead of the cohesive zone along the future crack path (which is of course possible only if the future path is known in advance).

The loading rate effect in crack band analysis has also been introduced for numerical purposes, as a mathematical means of preventing localization of strain-softening damage and achieving regularization of the boundary value problem without using a nonlocal model; see e.g. Sluys (1992) (with literature review). However, such studies did not deal with the problem of identifying a realistic material law for fracture growth in some particular material. The nonlinear viscoplastic effect on dynamic crack propagation was studied by Tvergaard and Needleman (1992), but not in the framework of the cohesive crack model.

The model presented in this paper is computationally simpler than that of Wu and Bažant (1993) in the sense that the use of compliance functions makes it possible to reduce the problem from two-dimensional to one-dimensional. The present model is also more realistic than that of Bažant and Jirásek (1993) because the cohesive stress distribution in the process zone in front of the crack tip is considered explicitly. The cohesive crack model is first formulated using the compliance functions (Green's functions) of the structure. Then the model is generalized to consider the linear viscoelastic behavior in the bulk of the material, including the aging which is typical of concrete. A nonlinear rate-dependent softening law is introduced into the stress-displacement law of the cohesive crack model. Special cases of the present model could also be applied to polymers, rocks and ceramics, and also to ice provided the nonlinear creep of ice is approximated linearly. Formulation of the computational algorithm, comparison to test results for concrete (including the response to a sudden loading rate change observed by Bažant and Gettu (1992), Bažant, Bai and Gettu (1993) and Bažant, Gu, Faber and Tandon (1995)) and studies of size effect are relegated to a subsequent companion paper (Li and Bažant, 1997).

2. Elastic cohesive crack model

The problem is considered to be two-dimensional and the structure to have a unit thickness $(b = 1)$. All the equations will be written for the case of plane stress. The equations for the case of plane strain may be obtained by replacing E with $E/(1 - \nu^2)$.

First, the well-known rate-independent cohesive crack model [e.g. Bažant and Li (1995)] needs to be briefly reviewed and its formalism defined. For a generic elastic structure, such as the three-point-bend fracture specimen shown in Figure 1a, we need to express the crack opening displacement $w(x)$ at a point x corresponding to the cohesive (or crack-bridging) stresses $\sigma(x')$ at other points x'.

For convenience of calculations, we consider that the crack extension line of the crack in the ligament up to point $x = a_n$ (Figure 1a) contains a preexisting cohesive crack of zero opening. This is admissible because a cohesive crack that has not yet started to open does not affect the
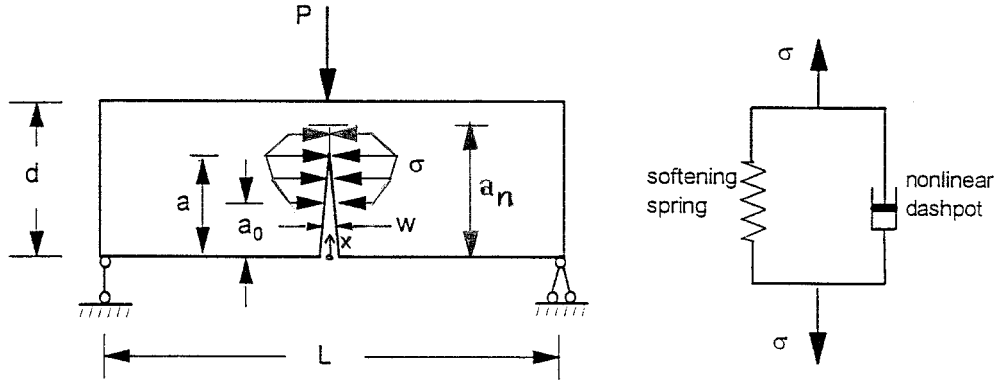
Figure 1. (a) Three-point-bent fracture specimen, (b) rate-dependent softening model.

stress and strain fields and is equivalent to no crack. The ultimate crack length a_n is chosen as the greatest length of the cohesive crack (including its cohesive zone) that is expected to occur in the calculations. The possibility to consider in calculations a crack of constant length a_n is an important advantage of the cohesive crack model (in the case of LEFM, a crack of variable length would have to be considered, which would greatly complicate the analysis). Of course, this approach is possible only if the crack path is known in advance.

According to the principle of superposition:

$$w(x) = - \int_{a_0}^{a_n} E^{-1} C^{w\sigma}(x, x')\sigma(x')\, \mathrm{d}x' + E^{-1} C^{wP}(x)P, \tag{1}$$

where E = Young's modulus, P = load or load parameter; a_0 = length of the initial traction-free crack or notch; $C^{w\sigma}(x, x'), C^{wP}(x)$ are the dimensionless compliance functions of the structure (with a crack of length a_n) calculated for a unit value of Young's modulus, $E = 1$. They may also be called the geometric compliance functions because they depend on the geometry of the structure, and particularly on the crack length a, but not on Young's modulus E. Note that $C^{w\sigma}(x, x') = C^{w\sigma}(x', x)$ because an elastic potential exists. Postulating a preexisting cohesive crack with a fixed crack length a_n has the advantage that the compliance functions do not change during the advance of the tip of the actual cohesive crack, which lies at $x = a$.

The stress in the cohesive crack model is everywhere finite. Thus, as proposed by Barenblatt (1959; 1962) and Dugdale (1960), the total stress intensity factor K at the tip $x = a$ of the process zone must be zero, that is $K = K_P - K_\sigma = 0$. This zero-K condition may be written as

$$k_P(a)P - \int_{a_0}^{a} k_\sigma(x; a)\sigma(x)\, \mathrm{d}x = 0, \tag{2}$$

in which $k_\sigma(x; a)$ = stress intensity factor at the process zone tip (located at a) due to a pair of unit forces acting on the crack surfaces at x, and $k_P(a)$ = stress intensity factor due to a unit load. Obviously, $k_\sigma(x; a) = 0$ for $x \geqslant a$. The tip of the process zone of the actual crack, $x = a$, is the point where the crack-bridging stress σ reaches the tensile strength f'_t of the material (Figure 1a).

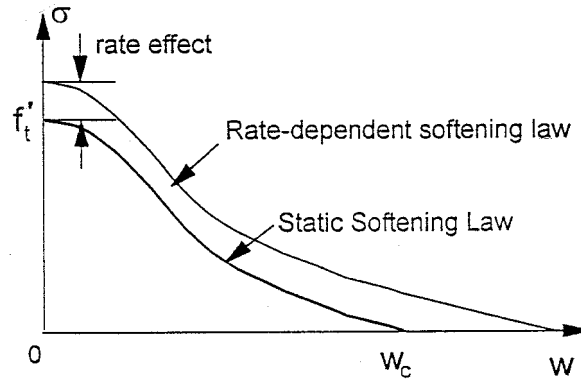*Figure 2.* Rate-independent and rate-dependent softening laws

In the static cohesive crack model, the cohesive (crack-bridging) stress σ is assumed to be uniquely related to the crack opening displacement w (Figure 2) according to the static softening law:

$$w = g(\sigma) \quad (0 \leqslant w \leqslant w_c, \quad 0 \leqslant \sigma \leqslant f_t'), \tag{3}$$

where g = monotonically decreasing function such that $g(f_t') = 0$ (the lowest curve in Figure 2); f_t' = tensile strength of the material and, for $\sigma \to 0$, $\lim g(\sigma) = w_c$ = threshold of w beyond which $\sigma = 0$ (Figure 2). Substituting (3) into (1), we obtain:

$$\text{for } 0 \leqslant x \leqslant a : \quad g[\sigma(x)] = -\int_{a_0}^{a_n} E^{-1} C^{w\sigma}(x, x')\sigma(x')\,dx' + E^{-1}C^{wP}(x)P$$
$$\text{for } a \leqslant x \leqslant a_n : \quad w(x) = 0 \quad \text{and} \quad \sigma(x) < f_t' \tag{4}$$

which is the crack compatibility equation. It expresses the condition that the crack opening calculated from the crack-bridging stresses and the softening stress-displacement law of the cohesive crack must be equal to (compatible with) the crack opening calculated from the given loads and the surface tractions acting on the surrounding elastic solid.

Equations (4) and (2) are the basic equations of the cohesive crack model. If a is given, P and $\sigma(x)$ can be solved from these equations. (Matrix finite element equations equivalent to a discrete approximation of (4) and (2) were directly introduced for concrete by Petersson (1981).)

Once P and $\sigma(x)$ are known for any a, then deformation at any point of the structure can be calculated, provided that the proper compliance functions have been determined. For instance, the crack mouth opening displacement (CMOD) can be expressed as

$$u = -\int_{a_0}^{a_n} E^{-1} C^{u\sigma}(x)\sigma(x)\,dx + E^{-1}C^{uP}P \tag{5}$$

$C^{u\sigma}(x)$ = opening displacement u at the crack mouth caused by a pair of unit forces acting on the crack surfaces at x, and C^{uP} is the opening displacement u at the crack mouth caused by a unit load $P = 1$, both being calculated for a unit value of Young's modulus E.

3. Viscoelastic cohesive crack model with rate-dependent crack opening

Consider now that the material, such as concrete, exhibits aging linear viscoelasticity, characterized by the compliance function $J(t, t')$, representing the strain at age t caused by a unit uniaxial stress applied at age t'. The aging of the material causes that $J(t, t')$ is a function of two variables t and t', and is not reducible to a function of one variable, the time lag $(t - t')$. For the purpose of triaxial generalization, it is convenient that, according to experimental results (for a review, see Bažant, 1988), the Poisson ratio can be assumed to be time independent (being equal to about 0.18). The structure is considered to be macroscopically homogeneous in the sense that the same $J(t, t')$ applies to every point of the homogenizing continuum throughout the bulk of the structure.

Since the actual crack of length a is mathematically equivalent to our preexisting cohesive crack of length a_n such that its portion from a to a_n is closed, the variation of the crack length $a(t)$ a function of time t does not prevent application of the elastic-viscoelastic analogy for aging structures (see, e.g., Bažant and Cedolin (1991), chapter 9, or Bažant (1988)). According to this analogy, the crack opening displacement w (as well as any displacement of the structure) can be obtained by replacing E^{-1} in Equation (1) for the elastic displacement by the aging viscoelastic operator defined by a linear Volterra integral equation (as explained, e.g., in Bažant (1988)). This leads to the expression:

$$w(x, t) = \int_{t_0}^{t} J(t, t') \bar{w}(x, \, \mathrm{d}t'). \tag{6}$$

Here t_0 is the time (or age) at which the load P is first applied and the first stresses are produced in the structure; $\bar{w}$ is the elastic crack-opening displacement calculated (from the stresses and loads) according to (1) for a unit value of Young's modulus ($E = 1$). The integral must be understood in the sense of Stieltjes, in order to allow integration over a jump of $\bar{w}$. The notation $\mathrm{d}t'$ in the argument of a function implies taking the differential or jump of the function only with respect to t'. For continuous dependence of $\bar{w}$ on t' (no jump),

$$\bar{w}(x, \, \mathrm{d}t') = \frac{\partial \bar{w}(x, t')}{\partial t'} \, \mathrm{d}t'. \tag{7}$$

If $\bar{w}$ has a jump at t_1 (which occurs when the load P changes instantaneously), the contribution to the integral in (6) from the infinitesimal interval (t_1^-, t_1^+) centered at t_1 is

$$J(t, t_1)[\bar{w}(t_1^+) - \bar{w}(t_1^-)]. \tag{8}$$

Introducing into (1) the dependence on time t, we have

$$\bar{w}(x, t) = -\int_{a_0}^{a_n} C^{w\sigma}(x, x') \sigma(x', t) \, \mathrm{d}x' + C^{wP}(x)P(t). \tag{9}$$

The increment of $\bar{w}$ at time t' may now be expressed as

$$\bar{w}(x, \, \mathrm{d}t') = -\int_{a_0}^{a_n} C^{w\sigma}(x, x') \sigma(x', \, \mathrm{d}t') \, \mathrm{d}x' + C^{wP}(x)P(\, \mathrm{d}t') \tag{10}$$

Substituting (10) into (6), we obtain the equation:

$$w(x, t) = -\int_{t_0}^{t} J(t, t') \int_{a_0}^{a_n} C^{w\sigma}(x, x') \sigma(x', \, \mathrm{d}t') \, \mathrm{d}x' + \int_{t_0}^{t} J(t, t') C^{wP}(x)P(\, \mathrm{d}t') \tag{11}$$

Because the zero-K condition (2) does not contain E, the elastic-viscoelastic analogy indicates this condition to remain valid even for the case of aging viscoelasticity.

Since the integration limits of the spatial integral in (11) are constant, it is possible to switch the order of spatial and temporal integrations. This leads to the following viscoelastic relation between the load history and the displacement:

$$w(x, t) = -\int_{a_0}^{a_n} C^{w\sigma}(x, x')\sigma_{\text{eff}}(x', t)\,\mathrm{d}x' + C^{wP}(x)P_{\text{eff}}(t) \quad \text{for} \quad t \geqslant t_0. \tag{12}$$

The quantities with the subscript 'eff' represent stresses and forces called 'effective'. They are defined as

$$\sigma_{\text{eff}}(x, t) = \int_{t_0}^{t} J(t, t')\sigma(x, \mathrm{d}t'), \quad P_{\text{eff}}(t) = \int_{t_0}^{t} J(t, t')\,\mathrm{d}P(t') \tag{13}$$

Note that while σ has the dimension of stress, σ_{eff} is defined as dimensionless. This agrees with the fact that J has the dimension of $(\text{stress})^{-1}$. Furthermore, σ_{eff} is dimensionless and P_{eff} has the dimension of m^2. Note that Equation (3) implies for the cohesive crack tip that $\sigma[a(t), t] = f'_t =$ tensile strength of the material.

We see that, in terms of the effective stresses and forces, the compatibility equation for the cohesive zone of the aging viscoelastic cohesive crack model is analogous to that of the time-independent cohesive crack model. This similarity is a manifestation of the elastic-viscoelastic analogy (or Biot's correspondence principle).

If the load $P(t)$ starts at t_0 by a discontinuous (instantaneous) jump from 0 to P_0 and then varies continuously, then the stresses on the cohesive crack and the crack line ahead of the crack tip make at t_0 an elastic jump from 0 to $\sigma(x, t_0)$ and then vary continuously. Then the Stieltjes integral may be expressed by means of the usual integral in the sense of Riemann as follows:

$$\sigma_{\text{eff}}(x, t) = J(t, t_0)\sigma(x, t_0) + \int_{t_0^+}^{t} J(t, t')\dot{\sigma}(x, t')\,\mathrm{d}t'$$

$$P_{\text{eff}}(t) = J(t, t_0)P(t_0) + \int_{t_0^+}^{t} J(t, t')\dot{P}(t')\,\mathrm{d}t', \tag{14}$$

where the superior dot denotes the time derivative, i.e. $\dot{\sigma}(x, t') = \partial\sigma(x, t')/\partial t'$; $\sigma(x, t_0) =$ stresses across the crack line caused by the first load $P(t_0)$ applied instantaneously at the time t_0 of the first loading.

Substituting the softening law (3) for w into (12), we obtain the following crack compatibility equation for an aging viscoelastic material:

$$\text{for } 0 \leqslant x \leqslant a: \quad g[\sigma(x, t)] = -\int_{a_0}^{a_n} C^{w\sigma}(x, x')\sigma_{\text{eff}}(x', t)\,\mathrm{d}x' + C^{wP}(x)P_{\text{eff}}(t)$$

$$\text{for } a \leqslant x \leqslant a_n: \quad w(x) = 0 \quad \text{and} \quad \sigma(x) < f'_t. \tag{15}$$

For the crack mouth opening displacement u (needed for analyzing fracture tests with the displacement control), application of the elastic-viscoelastic analogy to Equation (5) provides:

$$u(t) = -\int_{a_0}^{a_n} C^{u\sigma}(x)\sigma_{\text{eff}}(x, t)\,\mathrm{d}x + C^{uP}P_{\text{eff}}(t). \tag{16}$$

Instead of describing the aging viscoelasticity of the material by an integral equation, one can equivalently describe it by a system of differential equations corresponding to the Kelvin chain or the Maxwell chain (Bažant, 1988; 1995a). This is computationally advantageous when many nodes along the crack surface are chosen and when the problem is to be solved many times, as in the calculation of the size effect curves. The uniaxial constitutive relation based on the aging Kelvin chain can be written as:

$$\dot{\varepsilon} = \sum_\mu \frac{\dot{\gamma}\mu}{v_\mu(t)}, \quad \sigma = E_\mu(\gamma_\mu + \tau_\mu \dot{\gamma}_\mu) \quad (\mu = 1, 2, \ldots, N),$$ (17)

and that based on the aging Maxwell chain can be written as:

$$\sigma = \sum_\mu \sigma_\mu, \quad \dot{\sigma}_\mu + \frac{1}{\tau_\mu}\sigma_\mu = E_\mu v_\mu(t)\dot{\varepsilon} \quad (\mu = 1, 2, \ldots, N)$$ (18)

(Bažant, 1988, 1994; Carol and Bažant, 1993; and Bažant and Prasannan, 1989). Here a superior dot denotes the time derivative, γ_μ and σ_μ are the internal variables (hidden variables) corresponding to the strains or stresses in the individual Kelvin or Maxwell units (the partial strains or stresses), E_μ and τ_μ are the elastic moduli and the retardation or relaxation times of the units of the Kelvin or Maxwell chain, and v_μ are given positive functions, which increase at a decaying rate and define the aging of the material such as concrete (in which the aging is caused by the long-term chemical reactions of hydration of calcium silicates in Portland cement). We assume that the first relaxation or retardation time τ_1 is set to be extremely short, say $\tau_1 \approx 10^{-9}$s, so that the first Kelvin or Maxwell unit in the chain effectively represents elastic behavior. This makes it possible to write the subsequent equations more compactly. Most of the functions $v_\mu(t)$ can be assumed to be the same, particularly $v_\mu(t) = v(t)$ for $\mu = 2, 3, N - 1$. According to the solidification theory, $E_N(t) = 0$ for the last unit of Kelvin chain, which means that the unit degenerates into a dashpot of increasing viscosity $\tau_N E_N v_N(t)$. For details and generalization to general multiaxial stress, see (Bažant, 1988; Carol and Bažant, 1993; Bažant and Prasannan, 1989).

The transition from the linear elastic stress-strain relation $\sigma = E\varepsilon$ to the linear differential equation systems (17) or (18) defines a certain operation which involves the introduction of certain differential operators and the creation of internal variables (labeled by μ) associated with the kinematic or force variables of the problem (Bažant, 1994). The equations for creep can be obtained from the time-independent integral Equations (4) and (5) most easily by applying the same operation, which is in fact a manifestation of the elastic-viscoelastic analogy. This operation yields the following equations for the corresponding aging creep problem: for the Kelvin chain,

$$\dot{w}(x, t) = \sum_\mu \frac{\dot{w}_\mu(x, t)}{v_\mu(t)}, \quad \dot{u}(t) = \sum_\mu \frac{\dot{u}_\mu(t)}{v_\mu(t)},$$ (19)

$$E_\mu[w_\mu(x, t) + \tau_\mu \dot{w}_\mu(x, t)] = -\int_{a_0}^{a_n} C^{w\sigma}(x, x')\sigma(x', t)\, dx' + C^{wP}(x)P(t)$$

$$(\mu = 1, 2, \ldots, N),$$ (20)

$$E_\mu [u_\mu(t) + \tau_\mu \dot{u}_\mu(t)] = -\int_{a_0}^{a_n} C^{u\sigma}(x)\sigma(x,t)\,\mathrm{d}x + C^{uP}P(t)$$

$$(\mu = 1, 2, \ldots, N), \tag{21}$$

and for the Maxwell chain,

$$\sigma(x,t) = \sum_\mu \sigma_\mu(x,t), \quad P(t) = \sum_\mu P_\mu(t), \tag{22}$$

$$E_\mu v_\mu(t)\dot{w}_\mu(x,t) = -\int_{a_0}^{a_n} C^{w\sigma}(x,x';a)\left(\dot{\sigma}_\mu(x',t) + \frac{1}{\tau_\mu}\sigma_\mu(x',t)\right)\mathrm{d}x'$$

$$+C^{wP}(x)\left(\dot{P}_\mu(t) + \frac{1}{\tau_\mu}P_\mu(t)\right) \quad (\mu = 1, 2, \ldots, N), \tag{23}$$

$$E_\mu v_\mu(t)\dot{u}_\mu(t) = -\int_{a_0}^{a_n} C^{u\sigma}(x)\left(\dot{\sigma}_\mu(x,t) + \frac{1}{\tau_\mu}\sigma_\mu(x,t)\right)\mathrm{d}x$$

$$+C^{uP}\left(\dot{P}_\mu(t) + \frac{1}{\tau_\mu}P_\mu(t)\right) \quad (\mu = 1, 2, \ldots, N), \tag{24}$$

where a superior dot denotes the time derivative.

Equations (23) and (24) make possible an efficient recursive step-by-step integration algorithm, which does not require storing the history. The most efficient algorithm can be constructed using the general scheme of the exponential algorithm for concrete creep (Bažant, 1988; 1994). In this scheme, the recursive integration formulas for the time step are obtained by integrating the differential equations (19)–(24) exactly under the assumption that certain variables are constant within each time step and change only by jumps between the time steps. These are the variables $v_\mu(t)$, $P(t)$ and $\sigma(x,t)$ for the Kelvin chain, or $v_\mu(t)$, $\dot{u}_\mu(t)$ and $\dot{w}_\mu(x,t)$ for the Maxwell chain.

4.   Rate-dependent softening law for cohesive crack

Whereas for some materials, e.g., elastomers, it may suffice to consider viscoelasticity as the only source of the time-dependent fracture, for concrete and many other materials the fracture process itself must also be considered as rate dependent. In rocks and ceramics at room temperature, the latter may usually be considered as the only source of time-dependence (Bažant et al., 1993), but in concrete both sources of time dependence are important.

The rate dependence of the fracture process was initially described by a generalization of linear elastic fracture mechanics (LEFM) in which the growth rate of crack length a depends on the mode-I stress intensity factor K (Thouless et al., 1983; Evans and Fu, 1984; Schapery, 1980; Bažant and Prat, 1988), i.e., $\dot{a} = k_T(K/K_c)^n$ with the rate coefficient k_T given by an Arrhenius type equation $k_T = k_0 \exp(-Q/RT)$; k_0 and n = empirical constants, R = gas constant, T = absolute temperature, and Q = constant = activation energy. The Arrhenius type equation, justified by the rate-process theory for bond ruptures (Glasstone, 1941), was

introduced into LEFM-type fracture modeling by Zhurkov (1965; also Aleksandrov and Zhurkov, 1933; Cherepanov, 1979) and was proposed for the crack band and cohesive crack models in Bažant (1993). Because LEFM is inadequate for quasibrittle materials such as concrete, the simplest acceptable generalization for concrete is the R-curve model. Such a generalization has been formulated and experimentally validated by Bažant and Jirásek (1993).

As a further development, Bažant (1993; 1995a) derived from the activation energy theory (Glasstone, 1941) of the rate-process of bond ruptures on the atomic level (Appendix I) an equation that may be written as

$$\dot{w} = \dot{w}_0 \sinh\left(\frac{\sigma_b}{kf_t'}\right) \exp\left(\frac{Q}{RT_0} - \frac{Q}{RT}\right), \tag{25}$$

where $\dot{w}_0$ and κ are constants, $T_0 =$ chosen reference temperature, stress σ_b is a measure of the force per bond transmitted on the microscale by bonds that are being severed; $f_t' =$ tensile strength introduced to make κ dimensionless, and $\dot{w}_0 =$ reference crack opening displacement rate. At first it might seem questionable to deduce Equation (25) directly from the rate of rupture of atomic bonds, which represent a process on a far smaller scale. However, as far as the rates are concerned, such bridging of many scales is known to be admissible and has been successful in many other applications of the rate process theory (Evans and Fu, 1984; Glasstone et al., 1941). The basic assumption, which is quite obvious, is that if the process of atomic bond ruptures is accelerated, say, 1000-times, then the macroscopic fracture growth is also accelerated about 1000-times.

Based on experience, it is reasonable to assume that there exists a unique softening stress-displacement law for infinitely slow loading. We now use function $f(w)$ to denote this law, i.e., $\sigma - f(w) = 0$ for $\dot{w} = 0$. For increasing $\sigma - f(w)$, $\dot{w}$ must obviously increase. Therefore, as proposed in (Bažant, 1993), one may assume that $\sigma_b = \sigma - f(w)$. This is the simplest way to express the fact that, at constant σ, an increase of w must cause a decrease in the number of bonds per unit area, which in turn must cause an increase of the force per bond.

Because the long-time stress of concrete structures is known from experience to be about 80% of the short-time strength, Wu and Bažant (1993), in their finite element study, used function $f(w) = 0.8f_0(w)$ where $f_0(w)$ is the softening law that gives good results in normal-rate fracture tests. This also means that $f(0) \approx 0.8f_t'$ ($\approx$ long-time tensile strength f_t^∞).

For the case of constant temperature $T = T_0$, one arrives in this way at the following rate-dependent softening law (Bažant, 1993; Wu and Bažant, 1993):

$$\dot{w} = \dot{w}_0 \sinh\left(\frac{\sigma - f(w)}{\kappa f_t'}\right) \quad (\sigma \geqslant f(w)). \tag{26}$$

Equation (26) may preferably be written in the inverse form, which reads

$$w = g\left[\sigma - \kappa f_t' \operatorname{asinh}\left(\frac{\dot{w}}{\dot{w}_0}\right)\right], \tag{27}$$

where asinh is the inverse function of sinh and function g is inverse to f. Parameter κ, which normally ranges from 0.01 to 0.05 for concrete, determines the overall sensitivity of the softening law to change of crack opening rate. Parameter $\dot{w}_0$ (a constant) gives the value of loading rate below which the rate dependence becomes weak. Function $g(\sigma)$ characterizes the softening law of infinitely slow crack opening. Compared to the function $g(\sigma)$ that was

considered in the time-independent model for some particular narrow range of rates, function $g(\sigma)$ in (27) may be assumed they have a similar shape (except for the tail beyond w_c), but must be scaled down, as shown in Figure 2.

As illustrated in Figure 2, a change of opening rate $\dot{w}$ from one constant value to another causes, according to (27), a constant change to the argument of function $g(\sigma)$. Graphically, in Figure 2, this represents a vertical shift of the softening curve for the crack opening. Because of this shift, the definition of the static softening law must be extended into the region where $w > w_c$ as shown in Figure 2.

The sinh-type stress dependence of the crack opening rate given by (26) is highly nonlinear. Since the sinh-function approaches an exponential, the nonlinearity is equally pronounced at many orders of magnitude of the rate. This turned out to be an important aspect for successful modeling of concrete fracture (Bažant, 1993; Wu and Bažant, 1993). It was concluded that a viscoelastic-type relation between the crack-bridging stress and the crack opening can work only for one order of magnitude of the rate of loading, but not for many orders of magnitude.

In previous studies (Bažant, 1993; Wu and Bažant, 1993), Equation (26) was further refined as

$$\dot{w} = \dot{w}_0 \sinh\left(\frac{\sigma - f(w)}{\kappa f_t' + \kappa_1 f(w)}\right),\tag{28}$$

where κ_1 is a small positive constant. This modification makes it possible to control better the shape of a long tail of the softening stress-displacement curve. In the present study we use $\kappa_1 = 0$ because the precise shape of the tail, and in particular the extension of the softening law beyond w_c for $\dot{w} > 0$, is unimportant for the maximum loads.

5. Cohesive crack with rate-dependent opening

First, let us consider a cohesive crack with rate-dependent softening but without creep. The crack compatibility equation without creep may be generalized as

$$\text{for } 0 \leqslant x \leqslant a: \quad g\left\{\sigma(x, t) - \kappa f_t' \operatorname{asinh}\left(\frac{\dot{w}(x, t)}{\dot{w}_0}\right)\right\}$$

$$= -\int_{a_0}^{a_n} E^{-1} C^{w\sigma}(x, x')\sigma(x', t)\, \mathrm{d}x' + E^{-1} C^{wP}(x)P(t)\tag{29}$$

$$\text{for } a \leqslant x \leqslant a_n: \quad w(x) = 0 \quad \text{and} \quad \sigma(x) < f_t'.$$

The crack opening rate in this equation must now be expressed in terms of $\sigma(x, t)$ and $P(t)$. For this purpose, we differentiate Equation (1) with respect to time t, keeping in mind that a_n and the compliance functions are constant;

$$\dot{w}(x, t) = -\int_{a_0}^{a_n} E^{-1} C^{w\sigma}(x, x')\dot{\sigma}(x', t)\, \mathrm{d}x' + E^{-1} C^{wP}(x)\dot{P}(t).\tag{30}$$

The relation between the cohesive stress and the opening displacement may now be expressed as

$$w(x, t) = g\left\{\sigma(x, t) - \kappa f_t' \operatorname{asinh}\left(\frac{\dot{w}(x, t)}{\dot{w}_0}\right)\right\}\tag{31}$$

Although the material is assumed in this section to be elastic, the response of the model is history dependent because of the rate dependence of the softening law.

6. Cohesive crack with rate-dependent opening and aging creep

Finally, let us consider the most general case – both the rate-dependent softening in the crack and the aging creep in the surrounding material (concrete). To this end, function $g[\sigma(x, t)]$ in Equation (15) must be replaced by the rate-dependent expression (27). Thus, the crack compatibility equation takes the form:

$$\text{for } 0 \leqslant x \leqslant a : \quad g\left\{ \sigma(x, t) - \kappa f_t' \operatorname{asinh}\left(\frac{\dot{w}(x, t)}{\dot{w}_0} \right) \right\}$$

$$= -\int_{a_0}^{a_n} C^{w\sigma}(x, x')\sigma_{\text{eff}}(x', t)\, \mathrm{d}x' + C^{wP}(x)P_{\text{eff}}(t) \tag{32}$$

$$\text{for } a \leqslant x \leqslant a_n : \quad w(x) = 0 \quad \text{and} \quad \sigma(x) < f_t'.$$

Furthermore, we differentiate Equation (12) with respect to time t and obtain an equation similar to (30) except that σ is now replaced by $E\sigma_{\text{eff}}$. This furnishes for the crack opening rate the equation

$$\dot{w}(x, t) = -\int_{a_0}^{a_n} C^{w\sigma}(x, x')\dot{\sigma}_{\text{eff}}(x', t)\, \mathrm{d}x' + C^{wP}(x)\dot{P}_{\text{eff}}(t). \tag{33}$$

Note that the time derivatives of the effective stress and effective force appearing in these equations are not the same as their instantaneous elastic rates. For instance, the time derivative of σ_{eff} is

$$\dot{\sigma}_{\text{eff}}(x, t) = J(t, t)\dot{\sigma}(x, t) + \int_{t_0}^{t} \frac{\partial J(t, t')}{\partial t}\dot{\sigma}(x, t')\, \mathrm{d}t', \tag{34}$$

where the first term is the instantaneous elastic stress rate and the second term is the hereditary stress rate. The latter term represents the influence of viscoelasticity of the bulk material. Note that even if the actual stress rate is zero, the effective stress rate is not zero because of the contribution from the hereditary term. A similar expression applies for the time derivative of the effective load.

7. Characteristic length and scaling

The rate effects of creep are generally known to introduce an additional length scale into the mechanics of fracture or damage. Using a well-known algorithm (see e.g. (Bažant, 1988; Bažant and Prasannan, 1989)), one can expand the compliance function $J(t, t')$ into a Dirichlet series involving the retardation or relaxation times τ_μ of the units of the Kelvin or Maxwell chain, along with the corresponding spring moduli $E_\mu(t)$ (which depend on the age t of concrete); see (17), (18). In relation to the rate constant $\dot{w}_0$ of the crack softening law, these viscoelastic parameters introduce a series of age-dependent characteristic lengths:

$$l_\mu(t) = \dot{w}_0 \tau_\mu \frac{E_\mu(t)}{E(t_0)}, \tag{35}$$

where $E(t_0) = 1/J(t_0, t_0)$ = Young's modulus for the reference age of concrete, and G_f = fracture energy of the material, which is usually defined as the area under the softening stress-displacement curve (Hillerborg, 1976),

$$G_f = \int_0^\infty \sigma \, \mathrm{d}w = \int_0^{f_t'} g(\sigma) \, \mathrm{d}\sigma, \tag{36}$$

although it might be more reasonable to define it here as the area under the initial tangent of this curve (Bažant, 1996b). The fracture behavior is influenced by the ratios of these characteristic lengths to Irwin's characteristic size of the fracture process zone, which is

$$l_{\mathrm{ch}} = EG_f/f_t'^2. \tag{37}$$

Only those units of the Kelvin or Maxwell chain approximation whose characteristic length $l_\mu(t)$ is of the same order of magnitude as l_{ch} can cause a significant size effect on the fracture behavior, although the others still influence the viscoelastic response of the structure. This observation, however, does not bring about any simplification of the calculations reported in the next companion paper (Li and Bažant, 1997) because the actual compliance function, implying the full retardation spectrum, is used. ℓ_{ch} becomes irrelevant for structures so small that ℓ_{ch} is larger than the cross section dimension, and then the size effect must disappear.

8. Conclusion

In the time-dependent generalization of the cohesive crack model for concrete, one must take into account the fact that the time-dependence of fracture has two sources: the aging linear viscoelasticity (creep) in the bulk of the material and the rate dependence of the stress-displacement softening law for the crack-bridging stresses in the fracture process zone. As a realistic form of this rate dependence, a previously derived formula derived from the activation theory for bond ruptures is used.

A compact general formulation may achieved by using the compliance functions of the structure involving only the crack surface points and the loading point.

Together with the rate constants of the stress-displacement crack softening law, the retardation or relaxation times of the creep law introduce a set of additional characteristic length, whose comparison to the Irwin's characteristic size of the fracture process zone indicates the importance of the components of creep.

The formulation may also be applied to sea ice if the nonlinear creep of ice is approximated by linear viscoelasticity (without aging, which is a special case of the general formulation presented).

The subsequent companion paper will present a numerical algorithm for solving time-dependent fracture problems, compare the model predictions to the test data for concrete, study the roles of the different sources of time dependence, and explore the size effect.

Appendix I. Justification of sinh function for stress dependence of opening rate

For readers' convenience, a brief review of the basic result of the activation energy theory (Bažant, 1993) underlying Equation (25) will now be given. The fracture results from the ruptures of bonds between atoms or molecules. The atoms or molecules in solids are permanently in a random vibratory motion about their equilibrium positions representing the minimum

potential of the bond forces. The potential energy surface of the bond force exhibits maxima representing energy barriers called the activation energy, Q (Glasstone et al., 1941). If the maximum kinetic energy of the atom or molecule exceeds Q, the atom or molecule can jump over the activation energy barrier, which represents a rupture of the bond. The frequency of the jumps of atoms or molecules over their activation energy barrier Q controls the rate of the rupture process (it also controls many other processes, such as chemical reactions, diffusion, adsorption, creep, etc.). The statistical distribution of the thermal energies of atoms or molecules is well known. It follows from the Maxwell-Boltzmann distribution of thermal energies of atoms and reads

$$f = c_1 e^{-\varepsilon/RT}, \tag{38}$$

where f = frequency of attaining the energy level $\mathcal{E}$ at absolute temperature T, R = universal gas constant, and c_1 = constant.

The rate of fracture is assumed to be proportional to the frequency of bond ruptures, which is equal to the number of particles whose kinetic energy exceeds within a unit time a certain energy value $\mathcal{E}$ representing a material property. The potential energy barrier that needs to be overcome by the kinetic energy of one particle at zero applied stress is called the activation energy, Q. Under applied stress σ, the bond potential is modified with a gradient equal to σ superimposed on the potential energy diagram at zero stress (because the work of moving against the stress, per unit volume, is equal to σx). Therefore, the activation energy barriers against a particle making a jump along the stress direction or opposite to it are $\mathcal{E} = Q \pm \kappa\sigma$ (with κ = constant). Substituting this into (38), we get the frequency f_1 of exceeding the activation energy barrier for the jumps to the right which sever the bonds, and the jumps f_2 to the left which restore the bonds. Subtracting these two, we get the net frequency of bond ruptures as:

$$\Delta f = f_2 - f_1 = C_1 e^{(Q-\kappa\sigma_b)/RT} - C_1 e^{(Q-\kappa\sigma_b)/RT} \tag{39}$$

$$= C_1 e^{Q/RT}(e^{\kappa\sigma_b/RT} - e^{\kappa\sigma_b/RT}). \tag{40}$$

This result may be written as

$$\Delta f = C \sinh\left(\frac{\kappa\sigma_b}{RT}\right) e^{-Q/RT} \tag{41}$$

in which $C = C_1/2$ and κ, R = constants. Assuming $\dot{w}$ to be proportional to Δf, Bažant (1993) used this well-known result in deriving (25).

Appendix II. Time dependence of quasibrittle size effect

In relation to the preceding discussion of the characteristic length, it may be of interest to briefly outline a new approximate characterizations (Bažant, 1996a) of the size effect for structures with a large fracture process zone (or cohesive crack) subjected to sustained load.

The size effect on the maximum load $P_{\max}$ of a structure is commonly characterized by the nominal strength of the structure, defined as $\sigma_N = P_{\max}/bD$ (for the case of two-dimensional similarity) where D = structure size (characteristic dimension) and b = structure thickness at fracture front. For time-independent fracture of quasibrittle structures, the size effect may

be approximately described in fracture mechanics terms by the following formula derived in (Bažant and Kazemi, 1990a,b):

$$\sigma_N = \sqrt{\frac{EG_f}{g'(\alpha_0)c_f + g(\alpha_0)D}} = Bf_t' \left(1 + \frac{D}{D_0}\right)^{-1/2} \tag{42}$$

in which

$$D_0 = c_f \sqrt{\frac{g'(\alpha_0)}{g(\alpha_0)}}, \quad B = \sqrt{\frac{l_{ch}}{c_f g'(\alpha_0)}}. \tag{43}$$

Constant D_0 represents the size of transition from mainly ductile to mainly brittle response; $g(\alpha) = D(bK_I/P)^2$ = dimensionless LEFM energy release rate function characterizing the structure shape (geometry), K_I = stress intensity factor; $\alpha = a/D$ = relative crack length, $\alpha_0 = a_0/D$ = notch length or traction-free crack length; $g'(\alpha) = \mathrm{d}g(\alpha)/\mathrm{d}\alpha$; and c_f = nonlinear fracture parameter representing the effective length of the fracture process zone (or cohesive zone), defined for a structure size extrapolated to infinity (in which case the structure geometry becomes irrelevant). Equation (42) was amply verified by experiments and numerical simulation (Bažant and Kazemi, 1990a,b; Bažant, 1995; Bažant et al., 1994; and Bažant and Chen, 1997), was shown to approximate the size effect for the cohesive crack model, and was also derived by asymptotic matching (Bažant, 1997, 1995b).

A good approximate solution to concrete creep problems with sustained loading can usually be obtained from the elastic solution by replacing the elastic modulus E with the effective modulus $E_{ef} = 1/J(t,t') = E(t')/[1 + \phi(t,t')]$ where $E(t') = 1/J(t',t')$ = Young's modulus at age t' and $\phi(t,t') = E(t')J(t,t') - 1$ = creep coefficient (Bažant, 1988) {we must except from consideration, however, the long-time (many-year) response of concrete loaded at young ages (few weeks or months), for which a more refined concept, called the age-adjusted effective modulus, is required (Bažant, 1988)}. Making this replacement in expression (37) for the characteristic length, one concludes that creep should influence Irwin's characteristic length as follows (Bažant, 1996a):

$$l_{ch}(t,t') = \frac{G_f}{J(t,t')f_t'^2} = \frac{E(t')G_f}{[1 + \phi(t,t')]f_t'^2}. \tag{44}$$

This means that, if the material is viscoelastic, the characteristic size of the process zone decreases with load duration.

It now appears logical to assume that the effect of creep on the characteristic length of the fracture process zone, c_f, should be similar. So one may introduce the hypothesis that c_f in (43) should be replaced in the case of creep by the following time-dependent length:

$$c_{f_t} = \frac{c_f^0}{1 + \phi(t,t')}, \tag{45}$$

where c_f^0 = constant. Furthermore, one must note that, for sustained load, the tensile strength of concrete is a decreasing function $f'(t)$ of the duration of loading and, likewise, decreases with decreasing rate of loading. This decrease may be physically explained by the rate dependence of crack opening.

Thus it transpires that, for the case of creep, the parameters of the size effect law should be generalized as follows (Bažant, 1996a):

$$D_{0_t} = \frac{c_f^0}{1 + \phi(t, t')} \frac{g'(\alpha_0)}{g(\alpha_0)}, \quad Bf_t' = f_t'(t)\sqrt{\frac{l_{\text{ch}}^0}{c_f^0 g'(\alpha_0)}}, \tag{46}$$

where $l_{\text{ch}}^0 = G_f E(t')/[f_t'(t')]^2 =$ Irwin's length for short-time fracture. It appears that this simple viscoelastic generalization can describe quite well the test data in Bažant and Gettu (1992), which agree with the present cohesive crack model (Li and Bažant, 1995). However, a more extensive study is needed. It is beyond the scope of this paper and is planned for a follow-up paper.

Acknowledgment

References

Aleksandrov, A.P. and Zhurkov, S.N. (1933). *Yavlenie Khrupkogo Razryva* (The Phenomenon of Brittle Fracture). GTTI Press, Moscow.

Barenblatt, G.I. (1959). The formulation of equilibrium cracks during brittle fracture. General ideas and hypotheses. Axially-symmetric cracks. *Journal of Applied Mathematics and Mechanics (PMM)* **23**, 622–636.

Barenblatt, G.I. (1962). The mathematical theory of equilibrium cracks in brittle fracture. *Advances in Applied Mechanics* **7**, 55–129.

Barenblatt, G.I., Entov, V.M. and Salganik, R.L. (1970). Some problems of the kinetics of crack propagation. *Inelastic Behavior of Solids* (Edited by M.L. Kanninen et al.), McGraw-Hill, New York, 559–585.

Bažant, Z.P. (ed.). (1988). Mathematical modeling of creep and shrinkage of concrete. John Wiley, New York-Chichester, chapter 2.

Bažant, Z.P. (1993). Current status and advances in the theory of creep and interaction with fracture. *Proc. 5th International RILEM Symposium on Creep and Shrinkage of Concrete (ConCreep 5)* (held at U.P.C., Barcelona, September), (Edited by Z.P. Bažant and I. Carol, E and FN Spon), London, 291–307.

Bažant, Z.P. (1994). Creep and thermal effects in concrete structures: A conspectus of some new developments. Proc., *Computational Modelling of Concrete Structures (EURO-C)*, held at Innsbruck, Austria, March, Pineridge Press, 461–480.

Bažant, Z.P. (1995a). Creep and damage in concrete. *Materials Science of Concrete IV* (Edited by J. Skalny and S. Mindess), Am. Ceramic. Soc., Westerville, OH, 355–389.

Bažant, Z.P. (1995b). Scaling of quasibrittle fracture and the fractal question. *ASME Journal of Materials and Technology* **117**, 361–367.

Bažant, Z.P. (1996a). Internal research note, Northwestern University.

Bažant, Z.P. (1996b). Analysis of work-of-fracture method for measuring fracture energy of concrete. *ASCE Journal of Engineering Mechanics* **122**(2), 138–144.

Bažant, Z.P. (1997). Scaling of quasibrittle fracture: Asymptotic analysis. *International Journal of Fracture* **83**, 19–40.

Bažant, Z.P., Bai, S.-P. and Gettu, R. (1993). Fracture of rock: Effect of loading rate. *Engineering Fracture Mechanics* **45**, 393–398.

Bažant, Z.P. and Cedolin, L. (1991). *Stability of Structures: Elastic, Inelastic, Fracture and Damage Theories*, Oxford University Press, New York.

Bažant, Z.P. and Chen, E.-P. (1997). *Scaling of Structural Failure*. Report SAND96-2948–UC–703, Sandia National Laboratories, Albuquerque, New Mexico; also *Applied Mechanics Reviews ASME* **50**, (10), 593–627.

Bažant, Z.P. and Chern, J.-C. (1985). Concrete creep at variable humidity: Constitutive law and mechanism. *Materials and Structures* (RILEM, Paris), **18**, 1–20.

Bažant, Z.P. and Chern, J.-C. (1985). Strain-softening with creep and exponential algorithm. *Journal of Engineering Mechanics* ASCE **111** (EM3), 391–415.

Bažant, Z.P. and Gettu, R. (1992). Rate effects and load relaxation: Static fracture of concrete. *ACI Materials Journal* **89**(5), 456–468.

Bažant, Z.P., Gu, W.H. and Faber, K. (1995). Softening reversal and other effects of a change in loading rate on fracture of concrete. *ACI Materials Journal* **92**, 3–9.

Bažant, Z.P. and Jirásek, M. (1993). *R*-curve modeling of rate and size effects in quasibrittle fracture. *International Journal of Fracture* **62**, 355–373.

Bažant, Z.P. and Kazemi, M.T. (1990a). Determination of fracture energy, process zone length and brittleness number from size effect, with application to rock and concrete. *International Journal of Fracture* **44**, 111–131.

Bažant, Z.P. and Kazemi, M.T. (1990b). Size effect in fracture of ceramics and its use to determine fracture energy and effective process zone length. *Journal of American Ceramic Society* **73**(7), 1841–1853.

Bažant, Z.P. and Li, Y.-N. (1995). Stability of cohesive crack model: Part I–Energy principles. Trans. ASME. *Journal of Applied Mechanics* **62**, 959–964.

Bažant, Z.P. and Li, Y.-N. (1995). Stability of cohesive crack model: Part II–Eigenvalue analysis of size effect on strength and ductility of structures. Trans. ASME. *Journal of Applied Mechanics* **62**, 965–969.

Bažant, Z.P. and Oh, B.H. (1983). Crack band theory for fracture of concrete. *Material and Structures* **16**, 155–177.

Bažant, Z.P. and Ožbolt, J. (1990). Nonlocal microplane model for fracture, damage, and size effect in structures. *Journal of Engineering Mechanics* ASCE **116**(11), 2484–2504.

Bažant, Z.P., Ožbolt, J. and Eligehausen, R. (1994). Fracture size effect: review of evidence for concrete structures. *Journal of Structural Engineering ASCE* **120**(8), 2377–2398.

Bažant, Z.P. and Prasannan, S. (1989). Solidification theory for concrete creep. ASCE *Journal of Engineering Mechanics* **115**(8), 1691–1725.

Bažant, Z.P. and Prat, P. (1988). Effect of temperature and humidity on fracture energy of concrete. *ACI Materials Journal* **85**, 262–271.

de Borst, R. (1987). Smeared cracking, plasticity, creep and thermal loading - A unified approach. *Computer Methods in Applied Mechanics and Engineering* **62**, 89–110.

Carol, I. and Bažant, Z.P. (1993). Viscoelasticity with aging caused by solidification of nonaging constituent. *Journal of Engineering Mechanics*, ASCE, **119**(11), 2252–2269.

Cherepanov, G.P. (1979). Mechanics of brittle fracture. McGraw Hill, New York (translation from Russian, Nauka Press, Moscow 1974), 354–356.

Dugdale, D.S. (1960). Yielding of steel sheets containing slits. *Journal of the Mechanics and Physics of Solids* **8**, 100–104.

Evans, A.G. and Fu, Y. (1984). The mechanical behavior of alumina. *Fracture in Ceramic Materials*, Noyes Publications, Park Ridge, N.J., 56–88.

Freund, L.B. (1990). *Dynamic Fracture Mechanics*, Cambridge University Press, New York.

Glasstone, S., Laidler, K.J. and Eyring, H. (1941). *The Theory of Rate Processes*, McGraw Hill, New York.

Hillerborg, A., Modéer, R.M. and Petersson, P.-E. (1976). Analysis of crack formation and crack growth in concrete by means of fracture mechanics and finite elements. *Cement and Concrete Research* **6**, 773–782.

Hufferd, W.L. et al. (1975). On the fracture of viscoelastic materials. *CPIA Publications* **264**, 339–356.

Kanstad, T. (1990). *Nonlinear Analysis Considering Time-Dependent Deformation and Capacity of Reinforced and Prestressed Concrete*, Dr.-Ing. Dissertation, Norwegian Institute of Technology, University of Trondheim, Norway.

Knauss, W.G. (1970). Delayed failure – The Griffith problem for linearly viscoelastic materials. *International Journal of Fracture* **6**, 7–20.

Knauss, W.G. (1989). Time dependent fracture of polymers. *Advances in Fracture Research* **4**, 7th International Conference on Fracture, Houston, Texas, 2683– 2711.

Knauss, W.G. (1993). Time dependent fracture and cohesive zones. *Journal of Engineering Materials and Technology, Trans. ASME* **115**, 262–267.

Knauss, W.G. (1993). Crack propagation in a nonlinearly viscoelastic solid with relevance to adhesive bond failure. *Journal of Applied Mechanics ASME* **60**, 793–801.

Laheru, K.L. (1980). Crack growth initiation and propagation in inertly pressurized and in fired subscale rocket motors. *CPIA Publications* **331**, 267–279.

Li, Y.-N. and Bažant, Z.P. (1997). Cohesive crack model with rate-dependent crack opening and viscoelasticity: II. Numerical algorithm, behavior and size effect. *International Journal of Fracture* **86**, 267–288.

McCartney, L.N. (1988). Crack-growth predictions for viscoelastic materials exhibiting non-uniform craze deformation. *International Journal of Fracture* **37**, 279–301.

Nuismer, R.J. (1974). On the governing equation for quasi-static crack growth in linearly viscoelastic materials. *Journal of Applied Mechanics* ASME. **41**, 631–634.

Petersson, P.-E. (1981). *Crack Growth and Development of Fracture Zones in Plain Concrete and Similar Materials*, Doctoral Dissertation, Lund Institute of Technology, Sweden.

Schapery, R.A. (1975). A theory of crack initiation and growth in viscoelastic media. *International Journal of Fracture* **11**, 141–159.

Schapery, R.A. (1978). A method for predicting crack growth in nonhomogeneous viscoelastic media. *International Journal of Fracture* **14**, 293–309.

Schapery, R.A. (1980). Nonlinear fracture analysis of viscoelastic composite materials based on generalized J-integral theory. *Composite Materials* (Edited by K. Kawata and T. Akasaka), Japan Society for Composite Materials Tokyo, 171–180.

Schapery, R.A. (1982). Models for damage growth and fracture in nonlinear viscoelastic particulate composites. *Proc., 9th U.S. National Congress of Applied Mechanics*, Am. Soc. of Mechanical Engineers (ASME) Book No. H00228, 237–247.

Schapery, R.A. (1984). Correspondence principles as a generalized J-integral for large deformation and fracture analysis of viscoelastic media. *International Journal of Fracture* **25**, 195–223.

Schapery, R.A. (1989). On the mechanics of crack closing and bonding in linear viscoelastic media. *International Journal of Fracture* **39**, 163–183.

Sluys, L.J. (1992). *Wave Propagation, Localization and Dispersion in Softening Solids*, Dissertation, Delft University of Technology, Delft, The Netherlands.

Tada, H., Paris, P.C. and Irwin, G.R. (1985). Stress analysis of cracks handbook, Del Research Corp., Hellertown, Pa.

Tandon, S., Faber, K.T., Bažant, Z.P. and Li, Y.-N. (1995). Cohesive crack modeling of influence of sudden changes in loading rate on concrete fracture. *Engineering Fracture Mechanics* **52**(6), 987–997.

Thouless, M.D., Hsueh, C.H. and Evans, A.G. (1983). A damage model for creep crack growth in polycrystals. *Acta Metallurgica* **31**, 1675–1685.

Tvergaard, V. and Needleman, A.J. (1992). Effect of crack meandering on dynamic, ductile fracture. *Journal of the Mechanics and Physics of Solids* **40**, 447–471.

Tvergaard, V. and Hutchinson, J.W. (1992). The relation between crack growth resistance and fracture process parameters in elastic-plastic solids. *Journal of the Physics and Mechanics of Solids* **40**, 1377–1397.

Tvergaard, V. and Hutchinson, J.W. (1994). Effect of T-stress on Mode I crack growth resistance in a ductile solid. *International Journal of Solids and Structures* **31**, 823–833.

Williams, M.L. (1963). The fracture of viscoelastic material. *Fracture of Solids*, Interscience Publishers, New York.

Williams, M.L. (1964). Structural analysis of viscoelastic materials. *AIAA Journal*, 785–809.

Williams, M.L. (1965). Initiation and growth of viscoelastic fracture. *International Journal of Fracture* **1**, 292–310.

Willis, J.R. (1967). Crack propagation in viscoelastic media. *Journal of the Mechanics and Physics of Solids* **15**, 229–240.

Wu, Z.-S. and Bažant, Z.P. (1993). Finite element modeling of rate effect in concrete fracture with influence of creep. *Proc., 5th International RILEM Symposium on Creep and Shrinkage of Concrete (ConCreep 5)*, E & FN Spon, London, 427–432.

Zhou, F.P. (1992). *Time-Dependent Crack Growth and Fracture in Concrete*, Doctoral thesis, Report TVBM-1011, Lund, Sweden.

Zhurkov, S.N. (1965). Kinetic concept of the strength of solids. *International Journal of Fracture Mechanics* **1**(4), 311–323.

Cohesive crack model with rate-dependent opening and viscoelasticity: II. Numerical algorithm, behavior and size effect

YUAN-NENG LI* and ZDENĚK P. BAŽANT**
Department of Civil Engineering, Northwestern University, Evanston, Illinois 60208, U.S.A.

Abstract. In the preceding companion paper (Bažant and Li, 1997), the solution of an aging viscoelastic structure containing a cohesive crack with a rate-dependent stress-displacement softening law was reduced to a system of one-dimensional integro-differential equations involving compliance functions for points on the crack faces and the load point. An effective numerical algorithm for solving these equations, which dramatically reduces the computer time compared to the general two-dimensional finite element solution, is presented. The behavior of the model for various loading conditions is studied. It is shown that the model can closely reproduce the available experimental data from fracture tests with different loading rates spanning several orders of magnitude, and tests with sudden changes of the loading rate. Influence of the loading rate on the size effect and brittleness is also analyzed and is shown to agree with experiments.

Key words: Integro-differential equations in space and time, numerical algorithm, cohesive fracture, rate-effect, viscoelasticity, creep, quasibrittle materials, concrete, scaling, size effect, analysis of test data.

1. Introduction

A literature review and a model for a the rate-dependent cohesive crack in an aging viscoelastic structure have been presented in the preceding companion paper (Bažant and Li, 1995). This paper deals with the numerical implementation the model and its implications for size effect and brittleness. The use of compliance functions reduces the two-dimensional cohesive crack problem to one-dimensional integral equations. When the material is viscoelastic, the use of elastic-viscoelastic analogy makes it possible to preserve the one-dimensional form. Compared to the two-dimensional finite element formulations for concrete such as the rate-dependent crack band model proposed by Bažant (1983) (and applied by Wu and Bažant (1993)), the model of de Borst (1987), or the Gurson-type viscoplastic model of Tvergaard and Hutchinson (1994), the present one-dimensional compliance formulation is more efficient. The calculation of complete load-displacement curves by finite elements in two dimensions, which used to demand hours of devoted CPU time of a state-of-art workstation, is reduced to only a few minutes on the same machine.

The numerical method adopted in this paper is a generalization and modification of the algorithm used by Hillerborg et al. (1976) and Petersson (1981) for time-independent cohesive crack in an elastic structure. Unlike the general practice of numerical simulation of time-dependent phenomena, the time is not treated as an independent control variable. Instead, the crack length is selected as the control variable, and the corresponding time increment is solved. This approach is not only numerically more efficient but also more accurate, as long as the time dependence of all the relevant quantities is sufficiently smooth.

---

* Research Scientist in the Rank of Assistant Professor.
** Walter P. Murphy Professor of Civil Engineering and Materials Science.

The general behavior of the model will be studied for different loading rates and different specimen sizes. The change in the size effect curve caused by a change of loading rate will be also examined. The differene between the influences of viscoelasticity in the bulk material and of the rate-dependence of crack opening will be highlighted. Finally, comparisons with the relevant experimental results will be presented. Except for the labeling of dimensional and dimensionless variables, the notations from the preceding companion paper (Bažant and Li, 1997) will be retained.

2. Basic formulation

To facilitate the study of size effect, we will work with dimensionless variables. They may be defined as

$$w = \frac{f_t'}{G_f}\hat{w}, \qquad u = \frac{f_t'}{G_f}\hat{u}, \qquad P = \frac{\hat{P}}{Df_t'}, \qquad \sigma = \frac{\hat{\sigma}}{f_t'}, \qquad C = \frac{\hat{C}}{f_t'},$$

$$x = \frac{\hat{x}}{D}, \qquad \alpha = \frac{a}{D}, \qquad d = \frac{D}{l_0}, \qquad J(t,t') = E(t')\hat{J}(t,t'), \tag{1}$$

where $\hat{P} =$ applied load, $\hat{w} =$ crack-opening displacement, $\hat{u} =$ crack-mouth-opening displacement (CMOD), $\hat{x} =$ coordinate along the crack, $\hat{\sigma} =$ cohesive (crack-bridging) stress, $\hat{C} =$ any of the elastic compliance functions (or matrices) of the structure, $\hat{J}(t,t') =$ viscoelastic compliance function of the material; $f_t' =$ direct tensile strength, $E(t') =$ conventional (static) Young's modulus, $G_f =$ fracture energy of the material determined under the chosen reference loading rate (normally the rate of normal static test); $l_0 = EG_f/f_t'^2 =$ material length; $a =$ crack length; $D =$ characteristic size (dimension) of the structure (which is chosen, in our example, to represent the beam depth) and $b =$ structure thickness. All the other structural dimensions must be divided by D, and all the other displacements must be normalized by multiplying them by f_t/G_f. Because all the formulation will be given in the dimensionless form, we choose the dimensionless quantities (except D) to be unlabeled. Therefore we must label the actual quantities (except D), which is done by hats as written in (1), even though in the preceding companion paper the hats were not used for the actual quantities.

The compatibility equations for the general time-dependent cohesive crack model, presented in the preceding companion paper, may now be rewritten in the dimensionless form as follows

$$\frac{1}{D}g\left[\sigma(x,t) - \kappa \operatorname{asinh}\left(\frac{\dot{w}(x,t)}{\dot{w}_0}\right)\right]$$

$$= -\int_{\alpha_0}^{\alpha_n} C^{w\sigma}(x,x')\sigma_{\text{eff}}(x',t)\,dx' + C^{wP}(x)P_{\text{eff}}(t) \tag{2}$$

Also

$$\frac{u(t)}{D} = -\int_{\alpha_0}^{\alpha_n} C^{u\sigma}(x)\sigma_{\text{eff}}(x,t)\,dx + C^{uP}P_{\text{eff}}(t), \tag{3}$$

where $C^{w\sigma}(x, x')$, $C^{wP}(x)$, $C^{u\sigma}(x)$ and C^{uP} are the dimensionless forms of the elastic compliance functions introduced in the preceding companion paper, and $\alpha_n = a_n/D$. The zero-K condition may be written as

$$k_P P(t) - \int_{\alpha_0}^{\alpha_n} k_\sigma(x)\sigma(x, t)\, \mathrm{d}x = 0, \tag{4}$$

where k_P and $k_\sigma(x)$ are the stress intensity factors for crack tip at α due to a unit load or a pair of unit forces applied on the crack surfaces at x. They could also be made dimensionless but need not, because the equation is homogeneous.

The effective stresses and forces are calculated as

$$\sigma_{\text{eff}}(x, t) = \int_{t_0}^{t} J(t, t')\sigma(x, dt'), \qquad P_{\text{eff}}(t) = \int_{t_0}^{t} J(t, t')P(dt'), \tag{5}$$

where $J(t, t')$ is the non-dimensionalized viscoelastic compliance function of the material. For load durations up to one month, the creep of concrete is well described by the double power law proposed by Bažant and Chern (1985)

$$\frac{1}{E(t')}J(t, t') = \hat{J}(t, t') = \frac{1}{E_0}[1 + \phi(t'^{-m} + \alpha)(t - t')^n], \tag{6}$$

with $\phi = 3$ to $6, \alpha = 0.05, m = \frac{1}{3}$ and $n = \frac{1}{8}; t$ and t' must be given in days. Typically $E_0 = 1.5$ to $2E$ where E is the conventional static Young's modulus E. E_0 is constant (age-independent) and represents Young's modulus for instantaneous deformation corresponding to load durations extrapolated below 10^{-9} s. The present claculations use the values $\phi = 3.926$ and $E_0 = 18$ GPa. These values are selected under the condition that the effective Young's modulus at the peak load be equal to the conventional static Young's modulus, for which the loading rate causes the peak load of a reference size beam to be reached in about 10 minutes.

To analyze the rate-sensitive crack opening in an elastic structure, the effective stresses and forces are replaced by the actual stresses and forces, and the compliance function in Equation (5) is replaced by $1/E$. To analyze the effect of material viscoelasticity in a structure with a rate-insensitive crack opening, the term $\dot{w}$ in function g is discarded, i.e., $\dot{w} = 0$. In this way, different types of time-dependent fracture behavior can be studied using the same numerical algorithm.

3. Spatial approximation

The structure to be studied as an example is the three-point-bend beam shown in Figure 1(a). Due to its symmetry, only one half of the beam needs to be considered. The spatial approximation is achieved by the finite element method, using four-node bilinear elements. There are 90 elements across the beam depth, and an equal number of elements along the half beam span, with a gradually increasing element width.

The compliance functions are calculated by assigning a unit applied force at one node only and considering this force applied in turn at each point of the crack surface and at the loading point. The displacements at the crack surface nodes and at the load point calculated for each location of the unit applied nodal forces are then assembled into the compliance matrix $[C]$.
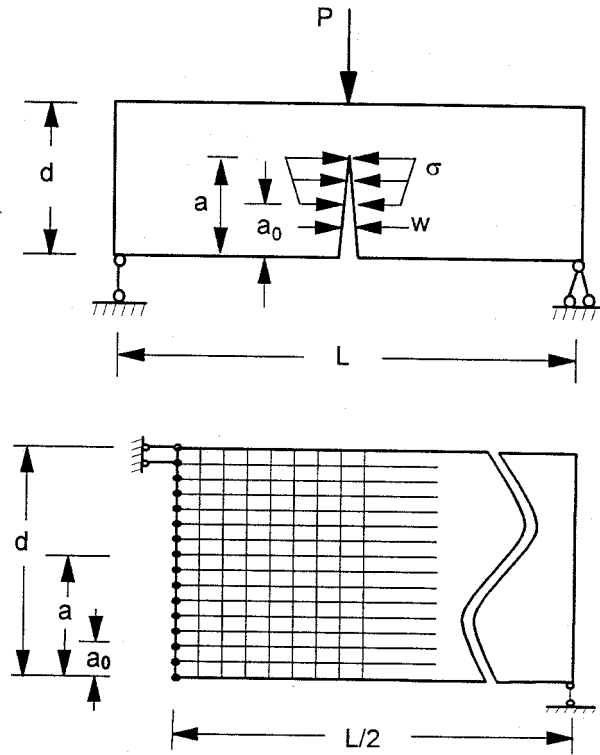
Figure 1. Geometry definition and finite element mesh of a three-point-bend beam.

First one calculates $[C]$ considering the crack to be as long as possible, with only a few elements left in the ligament. The corresponding elastic compatibility relation is then written in the matrix form as

$$\{w\} = [C]\{F\} + \{B\}P, \tag{7}$$

where $\{w\}$ is the column matrix of nodal crack-opening displacements, $\{F\}$ is the column matrix of nodal forces acting on the crack surface, and $[C]$ and $[B]$ are the compliance matrices that correspond to $C^{w\sigma}(x, x')$ and $C^{wP}(x)$. The compliance matrices corresponding to shorter cracks can be calculated from $[C]$ by prescribing zero opening displacements at the crack-tip node and the nodes ahead of the tip. The displacements are partitioned as $\{w\}^T = (\{w_1\}^T, \{w_2\}^T, \{w_3\}^T)$, where superscript T denotes the transpose; $\{w_1\} =$ displacements at traction-free crack nodes (coinciding initially with the nodes at notch surface); $\{w_2\} =$ displacements at the nodes in the cohesive (crack-bridging) zone; and $\{w_3\} =$ zero displacements in the ligament ahead of the cohesive crack tip. With a similar partitioning of $\{F\}$, $[C]$ and $\{B\}$, the foregoing elastic compatibility relation then reads

$$\begin{Bmatrix} \{w_1\} \\ \{w_2\} \\ \{w_3\} \end{Bmatrix} = \begin{bmatrix} [C_{11}] & [C_{12}] & [C_{13}] \\ [C_{21}] & [C_{22}] & [C_{23}] \\ [C_{31}] & [C_{32}] & [C_{33}] \end{bmatrix} \begin{Bmatrix} \{F_1\} \\ \{F_2\} \\ \{F_3\} \end{Bmatrix} + \begin{Bmatrix} \{B_1\} \\ \{B_2\} \\ \{B_3\} \end{Bmatrix} P. \tag{8}$$

By definition, $\{w_3\} = \{0\}$ and $\{F_1\} = \{0\}$; therefore, we can express $\{F_3\}$ in the ligament in terms of $\{F_2\}$ and P

$$\{F_3\} = -[C_{33}]^{-1}([C_{32}]\{F_2\} + \{B_3\}P).\tag{9}$$

Utilizing (9), one can express the matrix of crack-opening displacements in the process zone as

$$\{w_2\} = [C_{22}^*]\{F_2\} + \{B_2^*\}P,\tag{10}$$

where

$$[C_{22}^*] = [C_{22}] - [C_{23}][C_{33}]^{-1}[C_{32}], \qquad \{B_2^*\} = \{B_2\} - [C_{23}][C_{33}]^{-1}\{B_3\}.\tag{11}$$

The displacements in the notch can be written as

$$\{w_1\} = [C_{12}^*]\{F_2\} + \{B_1^*\}P,\tag{12}$$

where $[C_{12}^*] = [C_{12}] - [C_{13}][C_{33}]^{-1}[C_{32}]$ and $\{B_1^*\} = \{B_1\} - [C_{13}][C_{33}]^{-1}\{B_3\}$. In the experiment to be simulated later, the crack-mouth-opening displacement as a function of time t is given. Therefore, the first row of (12) is the discretized form of (3), which will be used later.

Note that column matrix $\{F\}$ represents the values of nodal forces, which is generally not the same as the nodal stress values. In the present calculations, it will be assumed that the cohesive stress is distributed linearly from node to node. The nodal forces corresponding to this assumption may be written in the form

$$\{F\} = [T]\{\sigma\},\tag{13}$$

where $[T]$ is a tridiagonal matrix. This relation is needed for both the cohesive zone and the ligament.

In the discrete approximation, the zero-K condition may be replaced by the condition that the stress value at the first node in the ligament must be equal to the tensile strength. According to the equilibrium condition, the column submatrix of nodal forces in the ligament may be expressed in (9) as

$$\{F_3\} = [T_{33}]\{\sigma_3\} + [T_{32}]\{\sigma_2\}.\tag{14}$$

The matrix $[T_{32}]$ has only one nonzero element because $[T]$ is tridiagonal. Therefore, upon mesh refinement, the term $[T_{32}]\{\sigma_2\}$ is higher-order small (proportional to element size) and could be neglected. This would, conveniently, yield $\{F_3\} \approx [T_{33}]\{\sigma_3\}$. However, instead of neglecting this term, the contribution from the nodal cohesive stresses, equivalent to $[T_{33}]\{\sigma_3\}$ but based on the previous loading stage, has been included directly in the equilibrium equation for the T-component for the cohesive crack-tip node. Thus, setting $\{F_3\} = [T_3]\{\sigma_3\}$ in (9) and inverting $[T_3]$, we can write the first matrix component equation in a dimensionless form as

$$(S_\sigma)\{\sigma\} + S_P P - 1 = 0,\tag{15}$$

where ( ) denotes a row matrix and $\{\sigma\}$ is the column matrix of the current nodal stress values in the cohesive crack zone corresponding to $\{w_2\}$. The subscript 2 is not used for $\{\sigma\}$ because $\{\sigma\}$ represents the main unknowns. All other quantities can be expressed in terms of $\{\sigma\}$.

Alternatively, the aforementioned handling of the term $[T_{32}]\{\sigma_2\}$ can be circumvented if the transformation from $\{F\}$ to $\{\sigma\}$ is done before the matrix partitioning. In that case, $\{F\} = [T]\{\sigma\}$ is substituted into (7), yielding

$$\{w\} = [\tilde{C}]\{\sigma\} + \{B\}P \quad \text{with } [\tilde{C}] = [C][T]. \tag{16}$$

Then the matrix $[\tilde{C}]$ rather than $[C]$ is partitioned along with $\{w\}$.

The discretized dimensionless compatibility equation for the process zone is given by (10). Dropping the subscripts and superscripts of the matrices, for the sake of simplicity, and keeping in mind the original definitions, we can write

$$\frac{1}{D}\left\{g\left(\sigma - k\,\text{asinh}\,\frac{\dot{w}}{\dot{w}_0}\right)\right\} + [\tilde{C}]\{\sigma_{\text{eff}}\} - \{\tilde{B}\}P_{\text{eff}} = 0, \tag{17}$$

where $[\tilde{C}] = [C_{22}^*][T_2]$ and $\tilde{B} = \{B_2^*\}$. The crack-mouth-opening displacement u must satisfy the relation

$$\frac{u(t)}{D} + (C_\sigma)\{\sigma_{\text{eff}}\} = B_P P_{\text{eff}} = 0, \tag{18}$$

where (C_σ) is the first row of $[C_{13}^*][T_2]$ and B_P is the first element of $\{B_1^*\}$.

4. New type of numerical algorithm: Controlled crack advance

In general, it would hardly be possible to solve the system of Equations (15)–(18) with the unknowns as continuous functions of time. Therefore, the finite difference method is introduced for the temporal discretization [3, 4].

To model the crack accurately, the tip of the cohesive crack must lie at the mesh node. However, for an arbitrary time step, the tip would generally reside somewhere between the mesh nodes, at different distances from the nodes in different time steps. Unfortunately, such a crack representation is rather inaccurate. It causes the response curves to be unsmooth. Improvement of accuracy would require certain interpolations between the nodes or a greatly refined discretization. This would complicate programming and extend computer time.

To overcome this problem, a new approach is proposed: The total crack length a is used as the basic control variable in the calculation and the crack tip is forced to always lie at a node. While in the conventional approach to static fracture the time step Δt and the increment Δu (say, CMOD) is prescribed, and the crack-length increment Δa and load increment ΔP are solved in each step, the presently proposed idea is to prescribe Δu and Δa, and solve Δt and ΔP.

Thus the time step Δt is treated as one of the unknowns to be solved. In each loading step of unknown duration Δt and a specified increment of CMOD, the cohesive crack tip is advanced by one node, i.e., the crack advance Δa is forced to be equal to the node spacing. In setting up the finite difference approximations for the time step, all the unknown variables are assumed to vary linearly with time within each time step.

This approach is attractive from the computational point of view, for two reasons. The first is that the order of accuracy of the temporal approximation can be matched to that of the spatial

approximation. The second is that much longer time steps than in the conventional approach can be used. This reduces the number of unknowns as well as the amount of computations and storage. The programming is thus simplified, and it becomes unnecessary to complicate programming by introducing the Kelvin or Maxwell chain approximation of creep.

Let t_0 be the time at which the load P is first applied to the structure, and t_i be the time at which the cohesive crack tip reaches the ith node along the crack path. The tip of the notch is numbered as the first node, $i = 1$. The rates of the cohesive stress and of the load are constant within each time step, according to our assumption. Thus the dimensionless effective stress is

$$\sigma_{\text{eff}}(x_i, t) = \sigma(x_i, t_0)J(t, t_0) + \sum_{j=0}^{n} \dot{\sigma}_i(t_j) \int_{t_j}^{t_{j+1}} J(t, \tau) \, d\tau, \tag{19}$$

where $J(t, \tau)$ = compliance function of the material = strain at time t caused by a unit uniaxial stress acting since time τ; $t_{n+1} = t$; $\sigma(x_i, t_0)$ = is the instantaneously produced first stress at point x_i; and $\dot{\sigma}_i(t_j)$ is the rate of dimensionless cohesive stress at node i during the time interval (t_j, t_{j+1}). The summation starts from i because, before t_i, the stress at node i is identically zero. A similar expression may be written for the effective load

$$P_{\text{eff}}(t) = J(t, t_0)P(t_0) + \sum_{j=0}^{n} P(t_j) \int_{t_j}^{t_{j+1}} J(t, \tau) \, d\tau. \tag{20}$$

These equations can be cast in a matrix form as

$$\{\sigma_{\text{eff}}\} = \{J\} + [\dot{\sigma}]\{H\}, \qquad P_{\text{eff}} = J(t, t_0)P(t_0) + (\dot{P})\{H\}, \tag{21}$$

where $\{J\}$ is the column matrix of the discrete values $J(t, t_i)$ corresponding to the first term on the right-hand side of (19), and H is the column matrix representing the values of the integral of the compliance function in the second term. $[\dot{\sigma}]$ is a square matrix representing the dimensionless stress rates, in which row i characterizes the stress rate history of node i and column j characterizes the nodal values of the stress rate profile during the time interval from t_j to t_{j+1}. $(\dot{P})$ is a row matrix representing the dimensionless load rate history.

The column matrix of the current values of the dimensionless stress and load can be expressed in terms of the matrices of the dimensionless stress and load rate histories

$$\{\sigma\} = \{I\} + [\dot{\sigma}]\{\Delta t\}, \qquad \{P_{\text{eff}}\} = \{P(t_0)\} + (\dot{P})\{\Delta t\}. \tag{22}$$

Here the jth element of the column matrix $\{\Delta t\}$ is $t_{j+1} - t_j$, and $\{I\}$ is a column matrix in which every element is 1.

With this formulation, the discretized system of (15)–(18) with (21) and (22) can be solved for a sequence of increasing crack lengths. For a given increase $\Delta \alpha$ of the total relative crack length α from node n to node $n + 1$ and a given increase Δu of CMOD, the unknowns to be solved are the current cohesive stress rate $\dot{\sigma}(t_n)$, the current loading rate $\dot{P}(t_n)$, and the time t_{n+1}.

In the solution procedure used here, two problems need to be handled. The first problem is to solve $\dot{\sigma}(t_n)$ and $\dot{P}(t_n)$ for an assumed value of time t_{n+1}, which is done from (15) and (17) using Newton's method (in which the solution obtained in the previous step may be taken as a very good initial guess of the solution for the current step). The second problem is to

determine t_{n+1} from (18), which is done by means of the secant method, with $u(t)$ as a known function of time. In this manner, the time rate of CMOD can be controlled.

To initialize the unknowns, t_1 and $\dot{P}(t_0)$ are solved from (15) and (18) considering $\{\sigma\} = \{0\}$ and $\{\sigma_{\text{eff}}\} = \{0\}$.

In the first problem, the column matrix of the nodal crack-opening rates is obtained from the equation

$$\frac{1}{D}\{\dot{w}\}(t_n) = -[C]\{\dot{\sigma}\}_{\text{eff}}(t_n) + \{B\}\{\dot{P}\}_{\text{eff}}(t_n). \tag{23}$$

When the bulk material is elastic, then subscript 'eff' can be dropped, and the stress rate and load rate can be used directly. When the material is viscoelastic, the effective stress rate and effective load rate are replaced by their finite difference approximations

$$\{\dot{\sigma}\}_{\text{eff}}(t_n) \approx \frac{\{\sigma_{\text{eff}}(t_{n+1})\} - \{\sigma_{\text{eff}}(t_n)\}}{t_{n+1} - t_n}, \qquad \dot{P}_{\text{eff}}(t_n) \approx \frac{P_{\text{eff}}(t_{n+1}) - P_{\text{eff}}(t_n)}{t_{n+1} - t_n}. \tag{24}$$

The controlled crack advance algorithm is not limited to structures with one concentrated load. An arbitrary system of loads evolving as a function of a single parameter P can be considered. The compliances and unit stress intensity factors must then of course be determined in reference to P as a parameter. Parameter P can depend on t and u.

REMARK. Instead of using the secant method to solve t_{n+1} from (18), as already mentioned, one could alternatively ontrol the time rate of CMOD by determining, for a given Δa, an approximate value of Δu that leads to the desired $\dot{u}$ according to the approximate estimator $\Delta u = \Delta a \dot{u}/[\Delta a/\Delta t]_{\text{old}}$, in which $[\Delta a/\Delta t]_{\text{old}}$ is the ratio obtained in the previous load step. The error introduced by delaying the enforcement of the prescribed displacement rate by one step is negligible, especially for a material such as concrete for which the response changes significantly only when the CMOD rate is changed by an order of magnitude. Improvement of accuracy is possible by iterating the loading step and taking the value of $[\Delta a/\Delta t]_{\text{old}}$ according to the solution obtained in the previous iteration.

5.   General behavior of time-dependent cohesive crack model

For numerical calculations, we consider three-point-bend fracture specimens (Figure 1). The span-to-depth ratio is 2.5. The ratio of the notch depth (initial crack length) to specimen depth D is $\frac{1}{6}$. Such specimens have been tested by Bažant and Gettu (1992). The crack mouth opening displacement u (CMOD) is controlled so as to keep its rate approximately constant.

Let the applied load be characterized by the dimensionless nominal stress $\sigma_N = 7.5\,P/d$ where P and d are the dimensionless load and the dimensionless structure size (Equation 1) and the factor 7.5 makes σ_N equal to the maximum bending stress in an uncracked beam. The stresses are divided by the tensile strength, f_t', and the displacements are divided by the threshold value of the crack-opening displacement, w_c, in order to make them dimensionless (Equation 1). The softening stress-displacement law for the cohesive crack is assumed to be linear

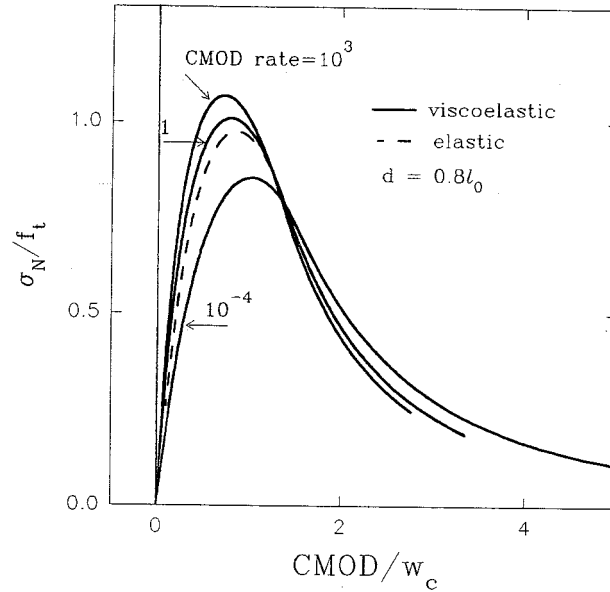$$g(\hat{\sigma}) = w_c\left(1 - \frac{\hat{\sigma}}{f_t'}\right), \tag{25}$$

Figure 2. Load-CMOD curves of cohesive crack model with viscoelasticity but no rate dependence of crack opening.

where w_c = constant = crack opening at which the cohesive stress is reduced to zero. (The solution for a nonlinear softening law could be obtained using the same numerical algorithm.)

Calculations show that the length of the stress-free portion of the crack remains initially equal to the notch depth. Later it extends farther, but usually only after the peak load.

First let us examine the effect of viscoelastic in the bulk material. It comes into play through the force-deformation relation. The deformation is determined by the effective forces, which depend on the entire loading history. The load-CMOD relation is plotted in Figure 2 for various loading rates. When the loading rate increases, the general trend is that, in the pre-peak region and shortly after the peak, the applied load becomes larger, while for the most part of the post peak region, the applied load becomes smaller, for the same CMOD value.

It is useful to use the size effect law proposed in 1983 by Bažant, which may be written in the form

$$\sigma_N = B f_t' \left(1 + \frac{D}{D_0}\right)^{-(1/2)}, \tag{26}$$

equivalent to (42) of the preceding paper (Bažant and Li, 1997). If this law is used to fit the experimental peak loads, then the parameter D_0 (representing the size at which the response changes from mainly ductile to mainly brittle) is found to decrease with a decreasing loading rate, as reported by Bažant and Gettu (1992). This phenomenon, which has been called the shift of brittleness (Bažant and Gettu, 1992) and is predicted by the analysis of the characteristic length in the preceding companion paper (Bažant and Li, 1997), implies that, for a slower loading rate, the material appears more brittle because brittleness must logically be defined as the proximity of failure behavior to the linear elastic fracture mechanics (LEFM) on the size effect curve. This observation, which agrees with the time dependence of D_{0_t} in the preceding companion paper (Bažant and Li, 1997), contradicts the intuitive perception of brittleness as
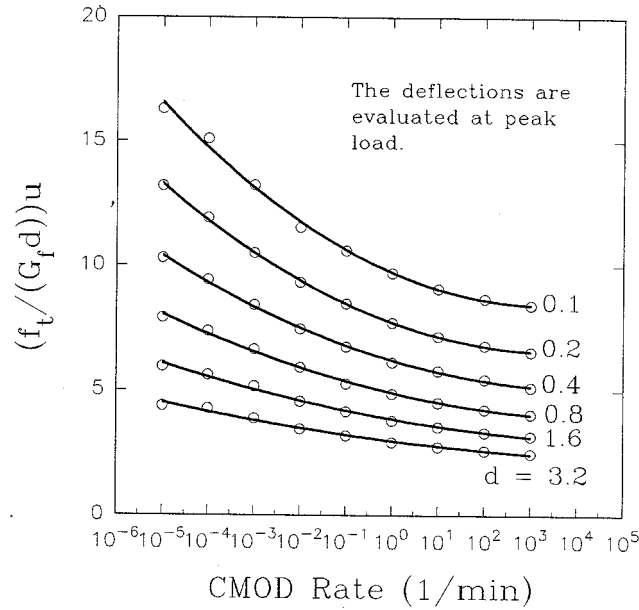
Figure 3. Load-line deflection at the maximum load as function of loading rate.
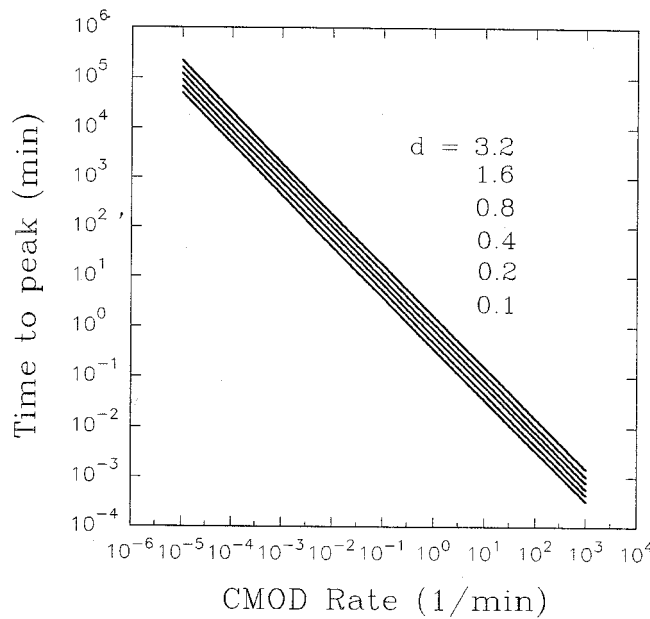

Figure 4. Time to peak versus loading rate for cohesive crack model with viscoelasticity but no rate dependence of crack opening.

the opposite of ductility, according to which the material may be seen as more ductile at a slower loading rate, due to more pronounced creep. The term 'brittleness shift' refers to the shift of the size effect curve closer to that for LEFM.

The deflections u (CMOD) under maximum load are plotted in Figure 3 for different specimen sizes as functions of the loading rate. The deflections are found to decrease with
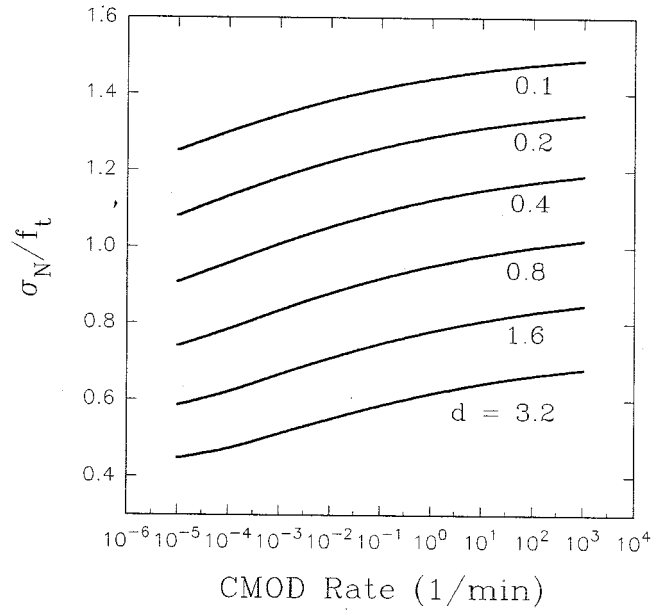
Figure 5. Rate effect on nominal strength according to cohesive crack model with viscoelasticity but no rate dependence of crack opening.
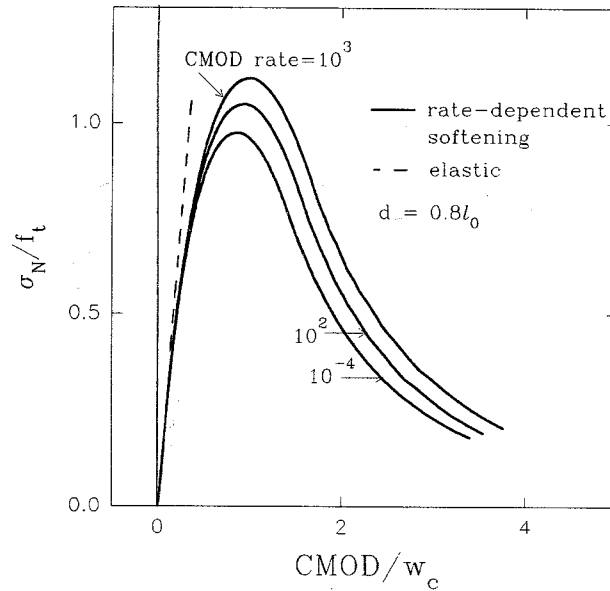
Figure 6. Load-CMOD curves of cohesive crack model with rate-dependent crack opening but no viscoelasticity.

an increasing loading rate, because the faster the load application, the smaller the creep. It is interesting that the time to peak load is an almost linear function of the loading rate in the log-log scale, as seen in Figure 4. The peak load as a function of the loading rate is plotted in Figure 5 for various specimen sizes. Note that these curves are approximately parallel to each other within the calculated range of the loading rates.
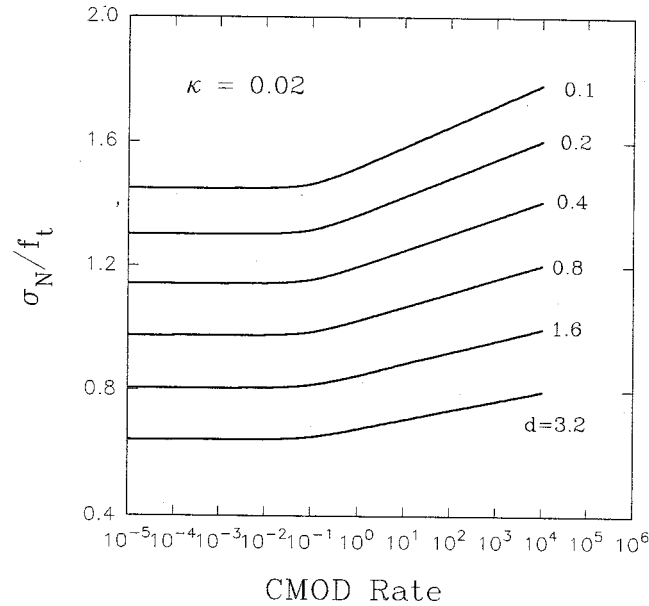
Figure 7. Rate effect on nominal strength of cohesive crack model with rate-dependent crack opening but no viscoelasticity.
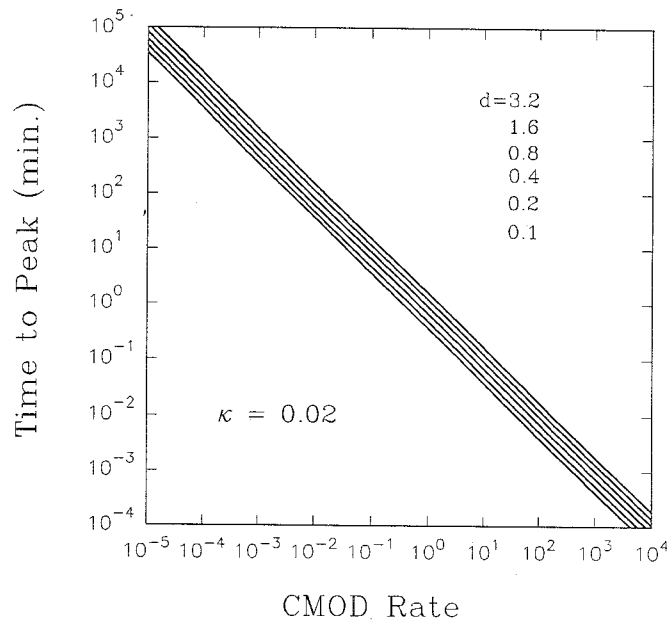

Figure 8. Time to peak versus loading rate for cohesive crack model with rate-dependent crack opening but no viscoelasitcity.

The behavior of the elastic cohesive crack model with a rate-dependent softening law is simpler than the behavior of the viscoelastic cohesive crack model. The rate dependence of the softening law comes into play when the rate of crack-opening displacement becomes significant. For a very slow loading rate, the response converges to the elastic solution, as
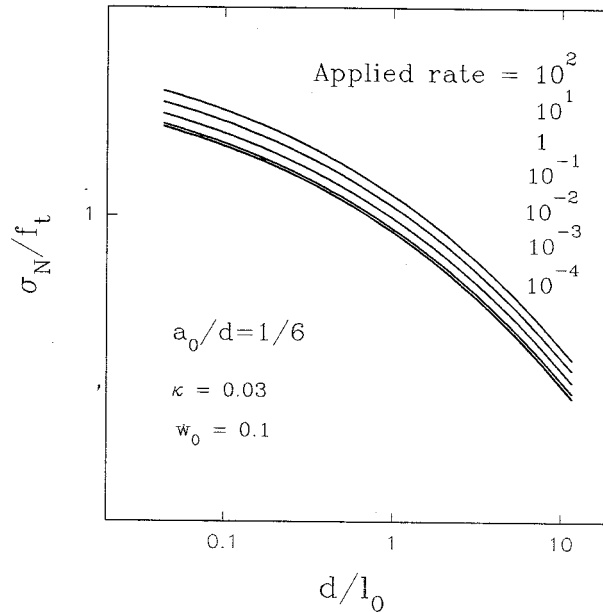
Figure 9. Size effect on nominal stress for viscoelastic cohesive crack model.

it can be seen from Figure 6 where the elastic curve (dashed) practically coincides with the curve for loading rate 10^{-4} m/min. Such a behavior can also be seen from Figure 7, where the peak load is plotted as a function of the loading rate for different specimen sizes. The curves for different sizes are almost parallel to each other. For very slow rates, the peak load curves become horizontal. This is rather different from what is displayed in Figure 5 because the compliance function for concrete creep (described here by the double power law) has no upper bound.

The time to peak as function of the loading rate is still linear on a log-log scale, as shown in model and might not be related to the rate dependence of the material properties. Further studies are needed to fully understand this behavior.

Qualitatively, the overall behavior of the viscoelastic cohesive crack model can be roughly understood through the concept of effective modulus, which is defined by the secant slope of the diagram of the nominal stress versus the dimensionless deflection at the peak load. As demonstrated by Figure 3, because of creep, the slower the loading rate, the larger the load-line deflection at peak. This means that a longer duration of the loading yields a smaller effective modulus. On the other hand, for very fast loading rates, the effective modulus increases because the viscosity becomes significant. Although the material toughness in terms of G_f is constant for these calculations (as the rate-dependent softening law is not used), the effective toughness in terms of K_f is rate-dependent because $K_f^2 = EG_f$ as well as E, which must be understood as the effective modulus, is rate-dependent. Consequently, the size effect curves of the viscoelastic cohesive crack model have different asymptotes for the large size limit. For a small size limit, the asymptote does not seem to change with the loading rate, since the plastic strength limit does not depend on the effective modulus.

For an elastic cohesive crack model with rate-dependent softening law, the size effect curves for different loading rates are parallel to each other, as shown in Figure 9. There are seven curves in the plot, but three of the curves, those for very slow loading rates, overlap each
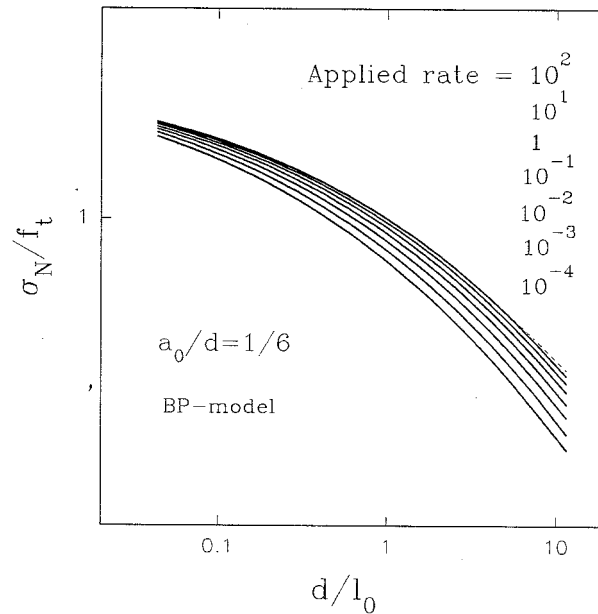
Figure 10. Size effect on nominal stress for cohesive crack model with rate-dependent crack opening but no viscoelasticity.

other. Since the softening curves are rate dependent, the material toughness and the material tensile strength are also rate dependent. As a result, the size effect curves for the small size limit and the large size limit have asymptotes that are mutually shifted while keeping the same slope. Although not shown in this paper, it is found that the fracture process zone (cohesive zone) length at the peak load is the same as for the cohesive crack model (which agrees with (46) of the preceding paper (Bažant and Li, 1997)). In other words, no change in the critical crack length is engendered by the rate dependence of the softening law.

For the viscoelastic cohesive crack model, the size effect and the rate effect interact. As shown in Figure 10, the increase in the dimensionless nominal stress is different for different dimensionless sizes when the loading rate increases by the same amount. The fracture process zone length at the peak load changes with the loading rate (roughly in agreement with (45) of (Bažant and Li, 1997)). As the loading becomes faster, the process zone length becomes longer, which is also manifested by a higher peak load value.

Comparing Figure 10 and Figure 9, we can see that there is virtually no brittleness shift in the elastic cohesive crack model with rate-dependent softening (which agrees with (46) of (Bažant and Li, 1997)). So we must conclude that the brittleness shift is caused mainly by viscoelasticity in the bulk material. We will return to this point later.

The size effect curves of the viscoelastic cohesive crack model with the rate-dependent softening law are given in Figure 11. The faster the loading, the more pronounced the size effect. To explain it, note that viscoelasticity of the material enhances the crack-opening rate, which in turn increases the cohesion between the crack surfaces. The rate-dependence of the softening law causes a uniform upward shift of the size effect curve when the loading rate becomes faster (as indicated by functions $f'_t(t)$ in (46) of (Bažant and Li, 1995)). This is the reason why the size effect curves are more widely spread out when compared with the size effect curves of the viscoelastic cohesive crack model.
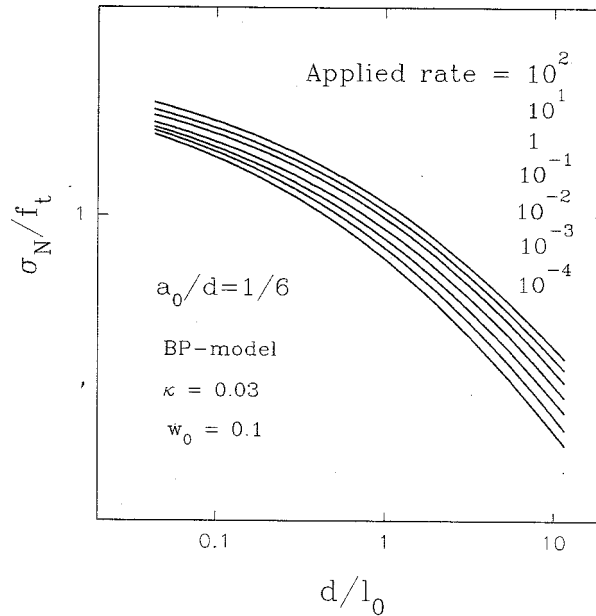
Figure 11. Size effect on nominal strength for cohesive crack model with both viscoelasticity and rate-dependent crack opening.

6. Behavior after a sudden change of loading rate

Comparing the rate effect curves for the viscoelastic cohesive crack model (Figure 5) to those for the elastic cohesive crack model with a rate-dependent softening law (Figure 7), one finds that, within a certain range of loading rates, the overall effects on the peak load for these two models are similar. In other words, it is difficult to distinguish the rate effect on the peak load from other effects if the range of the loading rate is not broad enough.

However, the test of a sudden change of loading rate, conducted by Bažant, Gu and Faber (1995) and Tandon et al. (1996), can separate the contributions to the rate effect arising from different mechanisms. If, in the post-peak range, the loading rate is greatly increased, for instance by three orders of magnitude, then the softening is found to change to hardening, followed by a second peak. Denote as P_0 the load level at which the loading rate is suddenly changed. Then, depending on the ratio of P_0 to the first peak load, P_1, the second peak (denoted as P_2) can be larger or smaller than the first peak.

The theoretical predictions of the curves of the applied load versus crack-mouth opening displacement (CMOD) under a sudden change of loading rate are plotted in Figure 12 for different models. The response for the elastic cohesive crack model is also included for the purpose of comparison. The responses of the model for a sudden increase and for a sudden decrease of the loading rate are plotted in Figure 12. The dimensionless size is chosen as 1.52, which roughly corresponds to the large specimen used in the Bažant and Gettu's experiments if the material length is taken to be 10 cm.

Figure 12(a) shows that the phenomenon of a second peak engendered by a sudden change of loading rate cannot be simulated by the viscoelastic cohesive crack model. The sudden change of loading rate causes only a slight change in the slope compared with the elastic
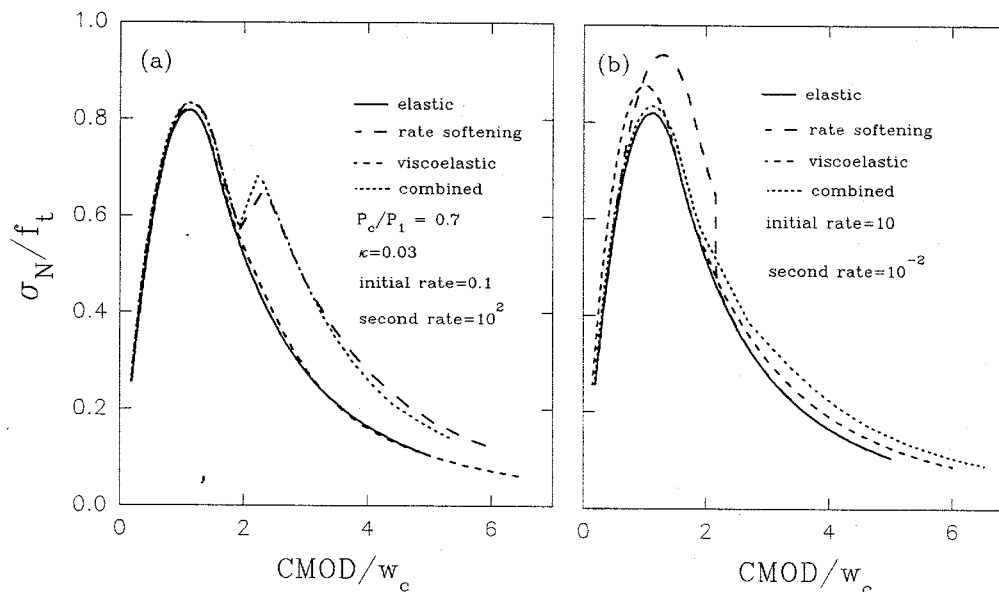
Figure 12. Calculated load-CMOD curves for (a) a sudden increase of loading rate and (b) a sudden decrease of loading rate.

cohesive crack model. The rate-dependence of the softening law is essential to obtain the second peak.

For a sudden decrease of the loading rate, the basic response is a sudden drop of the load, for all time-dependent cohesive crack models (as clearly seen in one case in Figure 12(b)). For the elastic cohesive crack model with a rate-dependent softening law, the response curve soon after the load drop becomes nearly coincident with the curve for a very slow constant-rate loading (the static curve). The viscoelastic cohesive crack model responds with a slight increase of the slope. This is because a decrease of the loading rate causes an increase of the load duration, which makes the creep deformation more pronounced. The viscoelastic cohesive crack model with rate-dependent softening responds with an increase of CMOD for the same level of load, which is similar to vsicoelastic cohesive crack model, but with a slightly higher loading level becuase the material is slightly stronger.

It is interesting to compare the responses at constant loading rate with those after a sudden change of loading rate. In Figure 13 there are four response curves of the viscoelastic cohesive crack model with rate-dependent softening, two of which are for constant CMOD rates of 10^{-2} m/min. and 10^{-4} m/min., respectively. The other two curves start with the rate 10^{-1} m/min. and then show the effect of an increase or sudden decrease of the rate by three orders of magnitude, taking place in the post-peak region at the point where the applied load has been reduced to 70 percent of the peak value. The CMOD rate changes are such that the final rates are the same as the previously considered constant rates. After the sudden change of CMOD rate, the curves for constant CMOD rates of the value are gradually approached. However, in contrast to the previous R-curve model (Bažant and Jirásek, 1993), they are not approached very closely.

The ratio P_2/P_1 is plotted in Figure 14(a) as function of P_0/P_1. After filtering out the random numerical scatter, one finds that the calculated response is basically a straight line independent of the specimen size D (denoted as d in the figures). This conclusion is similar to
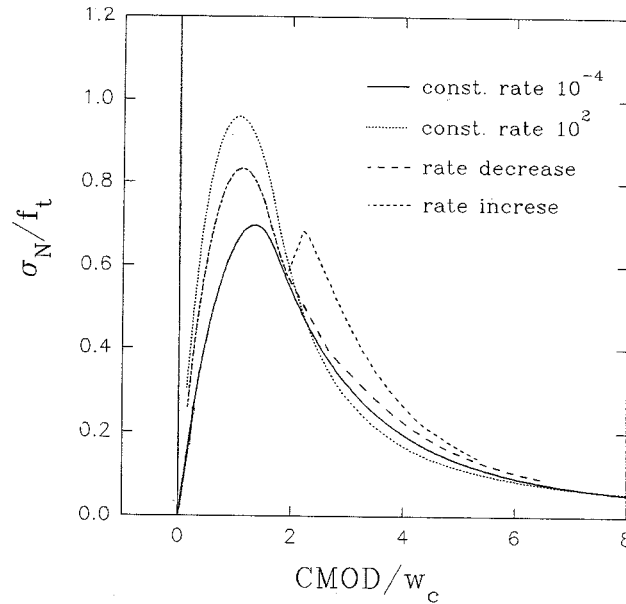
Figure 13. Comparison of the load-CMOD curves for loading with constant CMOD rate and with a sudden increase of loading rate by three orders of magnitude.
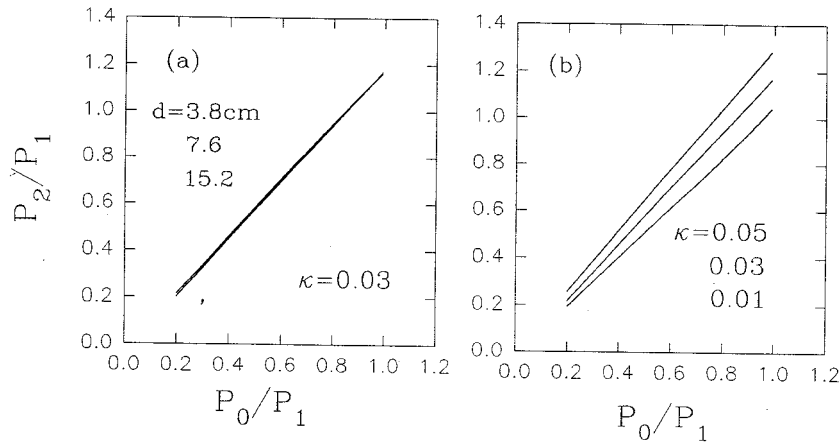

Figure 14. Second-peak on the load-deflection diagram for (a) different structure sizes and (b) different k values.

that obtained on the basis of the R-curve model by Bažant and Jirásek (1993), who obtained the same, virtually size-independent, plot. The greater the increase of the loading rate, the steeper the response curve. For a fixed increase of the loading rate, the actual location and the slope of the curve can be adjusted by the parameters of the present rate-dependent softening law.

As shown in Figure 14(b), the parameter κ determines the sensitivity of the model to the sudden loading rate change. The other parameter $\dot{w}_0$ has a similar effect on the second peak because these two parameters are not entirely independent of each other. A large $\dot{w}_0$ makes the model less sensitive to a sudden rate increase.
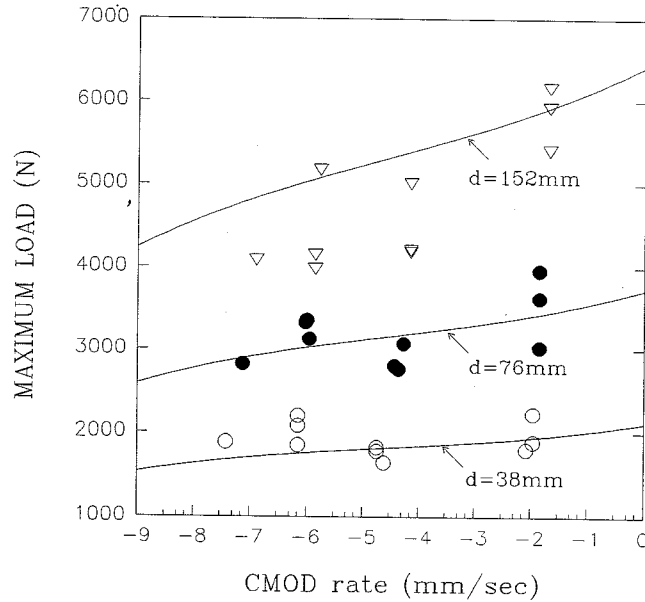
Figure 15. Comparison of rate effect on peak load with experimental data (size d is denoted as D in the text).

7. Comparison with experiments and empirical formulas

The theoretical prediction of the rate effect will now be compared with the experimental data on concrete by Bažant and Gettu (1992). The following material properties are used in the calculations: $f_t' = 3.75$ MPa, $l_0 = 0.16$ m, and $w_c = 30$ μm. For the rate-dependent softening law, the parameters are $k = 0.03$ and the reference rate is $\dot{w} = 100/$min.

The period of curing affects the strength of the concrete. According to the ACI recommendation, the concrete compressive strength at any age t (in days) can be calculated from the formula $f_c' = f_{c28}' t/(0.85t + 4.2)$ where f_{c28}' is the strength at 28 days. We will assume that the ratio of tensile strength of concrete at any age can be approximately calculated by the same formula. Thus the experimental values of the peak load are divided by the value $t/(0.85t + 4.2)$. In this, way the difference in curing ages of different test specimens is approximately taken care of. The comparison with test data is shown in Figure 15. It is satisfactory in view of the experimental scatter that is inevitable for concrete.

It is convenient to have a simple empirical expression for the rate-dependent size-effect curves. The generalized size-effect law proposed by Bažant (1985), which reads

$$\frac{\hat{\sigma}_N}{f_t'} = B \left[1 + \left(\frac{D}{D_0} \right)^r \right]^{-(1/2r)} \tag{27}$$

can fit, with a good precision, the numerical results of the viscoelastic cohesive crack model with a rate-dependent softening law. B, D_0 and r are rate-independent parameters, which can be determined by fitting the formula to the results of size effect tests (Bažant and Kazemi, 1990, and Bažant, 1993). The dimensionless parameter B determines the asymptotic strength value for very small structure sizes. One can express $D_0 = l_0 Z$ in which l_0 is a material property representing the material length defnined in (1) and Z depends only on the geometry of the specimen (Bažant and Kazemi, 1990, and Bažant, 1997). If the energy release rate is written as $G = \hat{\sigma}_N^2 \phi D/E$, then, in the large size limit, $Z = 1/(\phi B)$.

Table 1. Rate dependence of the empirical
parameters.

Rate (/min)	B	r	Z
10^{-4}	1.931	0.5549	0.3910
10^{-3}	1.942	0.5487	0.4729
10^{-2}	1.963	0.5348	0.5707
10^{-1}	1.976	0.5246	0.6728
10^0	1.989	0.5150	0.7768
10^1	1.997	0.5076	0.8759
10^2	2.004	0.5017	0.9667

For a softening law that is rate independent, parameter B represents the plastic limit. The plastic limit can be calculated as $(D - a_0)^2 f_t/2)$. For this estimate, we have $B = 2.083$. For the elastic cohesive crack model with a rate-dependent softening, however, it is found that the best fit is obtained for $r = 0.5131$, $Z = 0.7202$, and

$$B = 1.962[1 + \kappa \operatorname{asinh}(0.6\dot{u}/\dot{w}_0)], \tag{28}$$

where $\dot{u}$ (in 1 per minute) is the dimensionless CMOD rate (i.e., the CMOD rate divided by the crack-opening threshold value w_c). Note that for very slow loading rates, the optimum fit by (28) is very close to the estimated value of 2.083. This expression describes closely the numerically calculated size effect curves of the elastic cohesive crack model with a rate-dependent softening.

For the viscoelastic cohesive crack model, all the three parameters change with the rate. They can be approximately expressed by the following equations

$$B = 1.984(1 + 6.389 \times 10^{-3} \ln \dot{u}) \tag{29}$$

$$Z = 0.7711(1 + 0.1286 \ln \dot{u} + 8.6 \times 10^{-4} \ln \dot{u}) \tag{30}$$

$$r = 0.5162(1 - 0.0165 \ln \dot{u} + 8 \times 10^{-4} \ln^2 \dot{u}). \tag{31}$$

These expressions are valid only for $\dot{u}$ in the range approximately from 10^{-4} to 10^2. Within this range of rates, parameter B barely changes and is also very close to the estimated value 2.803. The change in r is also minor. The most significant change is associated with parameter Z which corresponds to the brittleness shift. Equations (31) are obtained on the basis of the data listed in Table 1. It is clearly seen that the shift of brittleness is related to viscoelasticity in the bulk of the material. If the viscosity of the material is insignificant, then the brittleness shift becomes undetectable, as has been already found by experiments (Bažant et al., 1993).

The rate-dependent size-effect curve of the viscoelastic cohesive crack model with rate-dependent softening can be represented by a combination of (28) and (31). Specifically, one can use the rate-dependent expressions for r and Z from (31) and calculate B according to the following equation

$$B = 1.984(1 + 6.389 \times 10^{-3} \ln \dot{u})[1 + \kappa \operatorname{asinh}(0.6\dot{u}/\dot{w}_0)]. \tag{32}$$

Table 2. Experimental rate-dependent parameters

Rate (/min)	Bf_t (MPa)/3.75	Old d_0 (m)	New d_0 (m)
Fast, 24	1.60	0.1030	0.124
Usual, 1.2×10^{-1}	1.68	0.0413	0.055
Slow, 2.4×10^{-3}	2.94	0.0131	0.0826
Very slow, 2.4×10^{-4}	3.47	0.0085	0.0658

This implies that contributions of the two time-dependent mechanisms, the viscoelasticity in the bulk material and the rate-dependent softening law in the crack process zone, are combined by simple multiplication.

The experimental data obtained by Bažant and Gettu (1992) were originally fitted by the size effect law (27) with Bf'_t and D_0 as free parameters, and r was kept to be 1. The calculated Bf'_t and D_0 are listed in Table 2. The values in the first column are the typical CMOD values used in experiments and calculated under the assumption that $w_c = 25\,\mu$m. The original values of Bf'_t listed in the second column correspond to 1/3.75 of the current value of Bf'_t because $\hat{\sigma}_N$, as defined in this paper, is 3.75 times larger than in de Borst (1987). Note that Bf'_t increases with a decreasing CMOD rate while D_0 increases in magnitude more than ten-times over the rate range studied. One must realize, however, that the tensile strength of concrete should not increase with a decreasing rate and, therefore, the fitting method should be modified. The tensile strength of concrete is assumed to be 2.75 MPa and $B = 2.083$, and the results of the new fitting are also listed in Table 2 (column 4). Note that the overall increase of D_0 is reduced to approximately a two-fold increase, which is basically the same as the theoretical prediction shown in Table 1. Furthermore, since D_0 by definition is equal to Zl_0, the predicted D_0 value can be approximately related to the new experimental D_0 value with $l_0 \approx 0.15$ m, which is a typical value for normal concrete used in the experiments (the optimum fit plotted in Figure 15 corresponds to $l_0 = 0.16$ m).

Further comparisons with experimental data on the load-CMOD curve after a sudden increase of the loading rate appear in a separate paper (Tandon et al., 1996).

8. Conclusions

(1) The smoothness of the numerically calculated response curves confirms that the proposed new numerical algorithm with controlled crack advance, in which the time step is solved such that the crack tip would always lie at a node, gives a consistent representation of fracture growth. If the crack tip were allowed to lie anywhere between the nodes, the response curves would be rough and a much finer discretization or more complicated programming would be needed.

(2) The attainment of good agreement with a broad range of test data confirms that the proposed rate-dependent cohesive crack model provides a realistic representation of the effects of material viscoelasticity and rate-dependence of crack opening. The present model correctly reproduces all the known basic types of behavior observed in experiments on concrete.

(3) The handling of viscoelastic response is gretaly simplified by using a constant compliance matrix for a crack that extends through the ligament and is longer than any actual crack

expected in the computations. The uncracked ligament ahead of the actual crack tip is represented as a cohesive crack that has not yet started to open. The tip of the actual crack is given by the point at which the cohesive (crack-bridging) stress reaches the value of the tensile strength of the material (this point and is also characterized by a zero value of the total stress intensity factor for the actual crack).

(4) By virtue of formulating the cohesive crack problem in terms of a compliance matrix for only the crack-surface nodes and the load point, the storage and computer time requirements for stress history in creep calculations are greatly reduced, compared to finite element solutions (Wu and Bažant, 1993) in which the unknowns for mesh nodes away from the crack surface are included. This facilitates programming and improves numerical efficiency. It allows handling situations where the fracture process zone is not small compared to the structure size and interacts with structure boundaries. The unknowns to be solved are the time step length and the stress rates at crack surface nodes, with the stress rate assumed to be constant within each time interval. The total crack length is prescribed to advance in each time step from one node to the next, which allows accurate representation of the crack. This new method contrasts with the conventional approach in which the length of time step is controlled. In that case the crack tip lies somewhere between the nodes, which makes accurate representation of the crack impossible.

(5) Some interesting features of the present model are revealed by computations. The logarithmic (log-log) plot of the time to peak versus the loading rate appears to be a straight line of negative slope. Although both aforementioned time-dependent mechanisms contribute to the increase of peak load with an increasing loading rate, their other effects are different:

  (a) The rate dependence of the softening relation of crack-bridging stress to crack-opening displacement causes a vertical shift of the size effect curve, but does not cause any brittleness shift (acceleration causes a shift upward). This rate dependence is the main reason why there is a reversal of slope of the load deflection curve and a second peak after a sudden increase of the loading rate in the post-peak region. Without this rate dependence, there would be no slope reversal. The fact that the rate dependence of the softening law does not cause an appreciable brittleness shift implies that it does not significantly affect the length of the cohesive (fracture process) zone (nor Irwin's characteristic length (Bažant and Li, 1997)).

  (b) Viscoelasticity in the bulk material causes a shift of brittleness in the sense that, in the size effect plot, the peak load solution moves closer to the asymptote for linear elastic fracture mechanics. The intuitive reason for this phenomenon, which is predicted by the analysis of the characteristic length in the preceding companion paper (Bažant and Li, 1997), is that viscoelastic stress relaxation in the material causes the cohesive zone length to decrease with a decreasing loading rate.

  (c) Viscoelasticity does not appear responsible for the phenomenon of slope reversal and second peak after a sudden increase of the loading rate.

  (d) The ratio of the second peak load to the first peak load as a function of the ratio of the load at which the rate is changed is independent of the specimen size.

(6) The peak loads calculated with the cohesive crack model can be represented with good precision by the approximate generalized size effect law proposed by Bažant (1985). The model allows a close match of the available experimental data on the rate and size dependence of the peak load, as well as the increase of brittleness caused by a decrease of the loading rate.

(7) The brittleness shift, i.e., the increase of brittleness for slower loading, is explained by the fact that the characteristic size l_{ch} of the farcture process zone decreases with time if the material creeps. The smaller the process zone, the more brittle the response.

Acknowledgment

References

Bažant, Z.P. (1985). Fracture mechanics and strain-softening in concrete. In *U.S.-Japan Seminar on Finite Element Analysis of Reinforced Concrete Structure* (held in Tokyo, published by *ASCE*, New York) **1**, 47–69.

Bažant, Z.P. (1993). Scaling laws in mechanics of failure. *Journal of Engineering Mechanics ASCE* **119**(9), 1828–1844.

Bažant, Z.P. (1995). Scaling of quasibrittle fracture and the fractal question. *ASME Journal of Materials and Technology* **117**, 361–367 (Materials Division Special 75th Anniversary Issue).

Bažant, Z.P. (1997). Scaling of quasibrittle fracture: Asymptotic analysis. *International Journal of Fracture* **83**(1), 19–40.

Bažant, Z.P., Bai, S.-P. and Gettu, R. (1993). Fracture of rock: Effect of loading rate. *Engineering Fracture Mechanics* **45**, 393–398.

Bažant, Z.P., and Chern, J.-C. (1985). Strain-softening with creep and exponential algorithm. *Journal of Engineering Mechanics ASCE* **111**(EM3), 391–415.

Bažant, Z.P., and Gettu, R. (1992). Rate effects and load relaxation: Static fracture of concrete. *ACI Materials Journal* **89**, 456–468.

Bažant, Z.P., Gu, W.-H., and Faber, K.T. (1995). Softening reversal and other effects of a change in loading rate on fracture of conrete. *ACI Materials Journal* **92**, 3–9.

Bažant, Z.P., and Jirásek, M. (1993). R-curve modeling of rate and size effects in quasibrittle fracture. *International Journal of Fracture* **62**, 355–373.

Bažant, Z.P., and Kazemi, M.T. (1990). Size effect in fracture of ceramics and its use to determine fracture energy and effective process zone length. *Journal of American Ceramic Society* **73**(7), 1841–1853.

Bažant, Z.P., and Li, Y.-N. (1997). Cohesive crack model with rate-dependent crack opening and viscoelasticity: Numerical method and behavior. *International Journal of Fracture*, **86**, 247–265.

Bažant, Z.P., and Oh, B.H. (1983). Crack band theory for fracture of concrete. *Material and Structures* **16**, 155–177.

Bažant, Z.P., Ožbolt, J. and Eligehausen, R. (1994). Fracture size effect: Review of evidence for concrete structures. *Journal of Structural Engineering ASCE* **120**(8), 2377–2398.

de Borst, R. (1987). Smeared cracking, plasticity, creep and thermal loading – A unified approach. *Computer Methods in Applied Mechanics and Engineering* **62**, 89–110.

Hillerborg, A., Modéer, M. and Petersson, P.-E. (1976). Analysis of crack formation and crack growth in concrete by means of fracture mechanics and finite elements. *Cement and Concrete Research* **6**, 773–782.

Petersson, P.-E. (1981). *Crack growth and development of fracture zones in plain concrete and similar materials*, Doctoral Dissertation, Lund Institute of Technology, Sweden.

Tandon, S., Faber, K.T., Bažant, Z.P., and Li, Y-N. (1996). Cohesive crack modeling of influence of sudden changes in loading rate on concrete fracture. *Engineering Fracture Mechanics* **52**(6), 987–997.

Tvergaard, V., and Hutchinson, J.W. (1991). Effect of T-stress on mode I crack growth resistance in a ductile solid. *International Journal of Solids and Structures* **31**, 823–833.

Wu, Z.S., and Bažant, Z.P. (1993). 'Finite element modeling of rate effect in concrete fracture with influence of creep', in Proc., 5th Intern. RILEM Symp. on Creep and Shrinkage of Concrete (ConCreep 5, held in Barcelona). Edited by J. Carol and Z.P. Bažant, E. and F.N. Spon, London 427–432.